NIST-GCR-90-573

ADSORPTION MODELING FOR MACROSCOPIC CONTAMINANT DISPERSAL ANALYSIS

FILE COPY
DO NOT TAKE

James W. Axley

Building Technology Program
Massachusetts Institute of Technology

Prepared for:
U.S. DEPARTMENT OF COMMERCE
National Institute of Standards
and Technology
Center for Building Technology
Indoor Air Quality and Ventilation Group
Building Environment Division
Gaithersburg, MD 20899

U.S. DEPARTMENT OF COMMERCE
Robert A. Mosbacher, Secretary
NATIONAL INSTITUTE OF STANDARDS
AND TECHNOLOGY
Dr. John W. Lyons, Director

NIST

NIST-GCR-90-573
Revised Sept. 1990

ADSORPTION MODELING FOR MACROSCOPIC CONTAMINANT DISPERSAL ANALYSIS

James W. Axley

Building Technology Program
Massachusetts Institute of Technology

Prepared for:
U.S. DEPARTMENT OF COMMERCE
National Institute of Standards
and Technology
Center for Building Technology
Indoor Air Quality and Ventilation Group
Building Environment Division
Gaithersburg, MD 20899

February 1990

Issued May 1990

U.S. DEPARTMENT OF COMMERCE
Robert A. Mosbacher, Secretary
NATIONAL INSTITUTE OF STANDARDS
AND TECHNOLOGY
Dr. John W. Lyons, Director

ABSTRACT

Two families of macroscopic adsorption models are formulated, based on fundamental principles of adsorption science and technology, that may be used for macroscopic (e.g., whole-building) contaminant dispersal analysis. The first family of adsorption models – the *Equilibrium Adsorption (EA) Models* – are based upon the simple requirement of equilibrium between adsorbent and room air. The second family – the *Boundary Layer Diffusion Controlled Adsorption (BLDC) Models* – add to the equilibrium requirement a boundary layer model for diffusion of the adsorbate from the room air to the adsorbent surface. Two members of each of these families are explicitly discussed, one based on the linear adsorption isotherm model and the other on the Langmuir model. The linear variants of each family are applied to model the adsorption dynamics of formaldehyde in gypsum wall board and compared to measured data.

1
INTRODUCTION

The dispersal of airborne contaminants and, thus, the quality of air in buildings is clearly dependent upon the nature of air movement into, out of, and within building systems and the character and location of contaminant sources. As a result, researchers in the field have focused on the complementary problems of modeling and measuring the airflow aspects of contaminant dispersal and the emission characteristics of contaminant sources. It is also well-recognized that some contaminants, such as Radon-222 gas and it's radioactive decay daughters and nitrogen dioxide, undergo chemical or radiochemical decomposition while being convectively transported by airflow and, therefore, modeling the dispersal of these contaminants demands the additional consideration of the chemical or radiochemical mass transformation processes involved.

It is not well-recognized, but has certainly been suspected, that adsorption and desorption processes can also significantly affect the dispersal of contaminants in building airflow systems. The evidence to support this suspicion is, however, pervasive. The lingering odors of winter clothes stored during the summer in the attic with mothballs, the familiar smell of grandparents home that persists for month's, even years, after their home remains vacant, the perfume-soaked blouse, and the noxious odor of clothes that were exposed to tobacco smoke or gasoline fumes that persists for days until washed. Few would doubt that adsorption and desorption phenomena can and do play a role in the dispersal of airborne contaminants in buildings but, from the point of view of indoor air quality analysis, should we suspect these phenomena to be significant? Can adsorption and desorption mass transport processes significantly alter the dynamics of the dispersal of indoor air contaminants? Under what circumstances should one suspect the effect to be significant and how may one rationally model the dispersal of a contaminant when these circumstances occur?

This report attempts to demonstrate that adsorption and desorption phenomena have not only the potential to significantly alter the dynamics of contaminant dispersal in buildings but may, in some cases, completely overwhelm the dynamics described by flow dispersal alone. Working from fundamental principles of the adsorption science literature, two families of adsorption/desorption models are formulated that provide a means to identify the circumstances under which sorption phenomena may come to be significant. It is shown that the simplest members of each of these families provide analytical models that appear to reliably predict indoor air quality dynamics when compared to measured data.

Some fundamental principles of adsorption science are presented in the second section of this report. Two families of single zone adsorption dynamics models are formulated in the third section and from the simplest member of each family two classes of adsorption element equations are extracted that may be used for general multi-zone contaminant dispersal analysis. Strategies to implement these using existing multi-zone contaminant dispersal analysis programs are also presented. The adsorption models are then applied to two problems of modeling the adsorption and desorption dynamics of formaldehyde in gypsum wall board, in the fourth section, corresponding to experimental tests conducted by researchers at Oak Ridge National Labs and the National Institute of Standards and Technology. Finally, in the fifth section conclusions are draw and some directions for additional studies are suggested.

2

FUNDAMENTALS OF ADSORPTION SCIENCE & TECHNOLOGY

Some fundamental ideas from the literature of adsorption science and technology will be reviewed here. Most of this literature is directed toward industrial applications of adsorption that involve the purposeful use of specially prepared adsorbents (e.g., activated carbon, zeolites, and synthetic resins) placed in adsorption devices (e.g., well-mixed batch reactors, well-mixed flow reactors, and fixed-bed reactors) that are carefully designed and controlled to achieve high rates of adsorption [11, 13, 14, 15, 16, 20]. The emphasis here, on the other hand, is directed toward modeling adsorption phenomena that is largely unintentional involving materials that tend to act as absorbents, but are not specially prepared to do so, that are placed in buildings for purposes other than that of adsorption separation. Given this emphasis we shall have to adapt ideas from the available literature and must limit our consideration to the simpler models of adsorption phenomena until additional study warrants the application (and provides the requisite data) of more complete adsorption models. An attempt will be made, however, to consider adsorption models that are sufficiently general to allow their application to modeling purposeful adsorption (e.g., indoor air purification) in building airflow systems.

Adsorption involves the separation of a substance from one phase, indoor air in the present context, and the accumulation of that substance on the surface of another phase, building materials, here. The nature of adsorption will depend on the nature of the adsorbent, the nature of adsorbate, and the interaction that may occur between them. After Slejko [20], we may distinguish four generic types of adsorption – exchange, physical, chemical, and specific adsorption. *Exchange adsorption* involves the exchange of one ionic species – the ionic adsorbate – with other ionic species attached to the surface of adsorbent and, therefore, involves electrostatic attraction of the adsorbate to the adsorbent. In *physical adsorption* the adsorbate is bound to the adsorbent by relatively weak intermolecular Van Der Waals forces. *Chemical adsorption* or *chemisorption* results from chemical reactions between the adsorbate and the adsorbent and, therefore, involves usually very strong binding forces associated with the sharing of electrons between the adsorbate and adsorbent. Finally, the term *specific adsorption* is reserved for adsorption phenomena involving binding of molecular groups, without chemical transformation, to specific functional groups on the adsorbent (e.g., polar adsorbates binding to polarized sites on the surface of an adsorbent). Specific adsorption binding forces fall in the spectrum between those for physical adsorption and chemisorption.

The nature of adsorption is directly linked to the strength of the forces that bind adsorbate to adsorbent with physical adsorption falling at the weak-force end of the spectrum and chemical adsorption at the strong-force end. With this in mind, it follows directly that:

a) adsorption is typically an exothermic process with the heat of adsorption associated with physical adsorption expected to be small relative to that associated with chemical adsorption,

b) physical adsorption may be expected to be a relatively reversible process while chemical adsorption may not, and

(c) chemical adsorption may be expected to be associated with the formation of a single layer of molecules of adsorbate on the surface of the adsorbent while in physical adsorption the possibility of multiple layers is more likely.

Reversibility and the heat of adsorption of a given adsorbate/adsorbent pair thus provide a direct indication of the molecular mechanism responsible for the adsorption.

Adsorption Equilibria

Physical and chemical adsorption processes may be more or less reversible[1] and can be represented as:

$$\text{Adsorbate} + \text{Adsorbent} \rightleftarrows \text{Adsorbate-Adsorbent Complex}$$

where the degree of reversibility depends, in part, on the thermodynamic state of the adsorbate-adsorbent system and the nature of bonding in the adsorbate-adsorbent complex. For physical adsorption the bonding is relatively weak and, thus, this reversible process may be thought, instead, to be a reversible exchange between two alternative phases of the adsorbate – the free or gas phase and the adsorbed phase – where the adsorbent may be thought to activate the phase transformation, not unlike a catalyst, rather than reacting to form a new adsorbate-adsorbent complex. Distinguishing the concentration of adsorbate near a surface, C^{*}, from that adsorbed on the surface, C_S, this reversible physical adsorption process may be represented as:

$$C^{*} \overset{\text{adsorbent}}{\rightleftarrows} C_S$$

where, for our purposes, concentration will be expressed in terms of mass fraction (i.e., the concentration in the air phase, C^{*}, will be expressed in terms of mass adsorbate per mass of the gas phase (e.g., mass adsorbate/mass of air) while the concentration in the solid phase, C_S, will be expressed in terms of mass adsorbate per mass of solid adsorbent[2]).

---

[1] For chemical adsorption reversibly may demand elevated temperatures.

[2] The concentration of adsorbate adsorbed on the surface is sometimes expressed in terms of mass adsorbate per unit of specific surface area of the adsorbent or, in indoor air quality literature, in terms of mass adsorbate per unit of projected surface area of the adsorbent (e.g., wall surface area). Effective adsorbents typically have extremely large specific surface areas due to convoluted surfaces and porosity. The specific surface area of an adsorbent may be difficult to determine and may not be well correlated to projected surface area, hence, it is practically more

Under isothermal conditions the rate at which adsorbate molecules (or ions) are adsorbed, in a closed system, will eventually equal the rate at which they are desorbed, a state of equilibrium will be achieved, and the concentration in each phase will remain constant at their respective equilibrium values, C_e^* and C_{Se}. The equilibrium surface concentration generally increases with the equilibrium gas phase concentration for a given isothermal condition. The variation of this concentration, C_{Se}, with the gas equilibrium concentration, C_e^*, for a given state of temperature, is commonly called an *adsorption isotherm*. Experimentally determined adsorption isotherms, typically represented graphically, may be approximated by one of several equilibrium models including the Linear Model, Langmuir Model, BET Model, and Freundlich Model; the first three having theoretical bases and the last being empirical.

Linear Model: This adsorption isotherm is defined by a simple linear relationship:

$$C_{Se} \equiv K_P\, C_e^* \tag{2.1}$$

where K_P is a temperature-dependent coefficient known as the *Henry adsorption constant*[3] or the *partition coefficient* [16, 20]. This single parameter (i.e., K_P) model may be expected to be appropriate for cases of physical adsorption of gases at very low concentrations (e.g., trace amounts) on homogeneous surfaces with ample sites available for adsorption.

Langmuir Model: In the years 1916-1918 Langmuir developed an adsorption isotherm model that accounted for the fact that the sites available for adsorption are limited [16, 20]. The Langmuir model may be expressed, for our purposes, as:

$$C_{Se} \equiv \frac{C_{So}\, K_L\, C_e^*}{1 + K_L\, C_e^*} \tag{2.2}$$

where C_{So} is the surface concentration corresponding to complete coverage by a single monolayer (constant, for a given adsorbate-adsorbent system, and independent of temperature for the Langmuir assumption of a fixed number of sites available for adsorption) and K_L is the temperature-dependent *Langmuir adsorption coefficient.*

The Langmuir model approximates the linear model for very low concentrations of adsorbate in the gas (or liquid) phase (i.e., when $K_L\, C_e^* << 1$) thus we should expect near equality between the partition coefficient and the product of the parameters of this model as:

---

convenient to employ mass fraction.

[3] Henry's Law defines a linear, equilibrium relation between the vapor pressure of a slightly soluble gas and its concentration in liquid solution. By analogy to this gas solution process the linear model for adsorption is sometimes called Henry's Law.

$$K_P \approx C_{So} K_L \tag{2.3}$$

BET Model: Brunauer, Emmett, and Teller developed a model that accounted for the possibility of multilayer adsorption that may be expected to occur in physical adsorption [16]:

$$C_{Se} \cong \frac{C_{So} K_{BET}\left(C_e^*/C_{sat}^*\right)}{\left(1 - \left(C_e^*/C_{sat}^*\right)\right)\left(1 - \left(C_e^*/C_{sat}^*\right) + K_{BET}\left(C_e^*/C_{sat}^*\right)\right)} \tag{2.4}$$

where K_{BET} is the BET constant related to the energy of adsorption and C_{So} is the surface concentration corresponding to complete coverage by a single monolayer (constant for a given adsorbate-adsorbent system) and C_{sat}^* is the air phase concentration corresponding to saturated conditions. The BET model has been found to be reliable in the range of reduced concentrations of $0.05 < \left(C_e^*/C_{sat}^*\right) < 0.35$ [16] for many gas adsorbate-solid adsorbent systems.

The BET model also approximates the linear model for very low concentrations of adsorbate in the gas (or liquid) phase:

$$\left(C_e^*/C_{sat}^*\right) << 1 \quad \text{and} \quad K_{BET}\left(C_e^*/C_{sat}^*\right) << 1$$

thus we should expect near equality between the partition coefficient and the product of the parameters of this model as:

$$K_P \approx \left(C_{So} K_{BET}/C_{sat}^*\right) \tag{2.5}$$

Freundlich Model: An alternative two parameter model that often fits experimental data well was promoted by Freundlich [20]:

$$C_{Se} \cong K_F C_e^{*(1/n)} \tag{2.6}$$

where K_F and n are the constant parameters associated with the Freundlich model.

From a somewhat simplified consideration of adsorption thermodynamics it may be shown that the temperature dependency of the adsorption coefficients used in the Linear, Langmuir, and BET models may be expected to be described by Arrhenius type relationships [16, 20]:

$$K_P \cong K_{Po} e^{-\Delta H/RT} \tag{2.7a}$$

$$K_L \cong K_{Lo} e^{-\Delta H/RT} \tag{2.7b}$$

$$K_{BET} \cong K_{BETo} e^{(E_1 - E_2)/RT} \tag{2.7c}$$

where,

a) K_{Po}, K_{Lo}, and K_{BETo} are constants, ΔH is the enthalpy change associated with adsorption (J/kmol), and E_1 is the average heat of adsorption of the first layer adsorbed which depend on the particular adsorbate-adsorbent system being considered,

b) E_2 is the heat of condensation of the adsorbate, and

c) R is the universal gas constant (8314.4 J/kmol-°K), and T is absolute temperature (°K) at which a given adsorption isotherm is defined.

A plot of the logarithm of experimental determined model constants $\log(K_P)$, $\log(K_L)$, or $\log(K_{BET})$ versus 1/T provides an indication of the correctness of the particular model (i.e., it should be a straight line) and provides a means to evaluate the Arrhenius constants. Borrazzo recently reported this to be so for some nine hydrocarbons commonly found in indoor air adsorbed on nylon, wool, and glass fibers [1].

3

ZONE ADSORPTION DYNAMICS

In this section we shall adapt some of the principles of adsorption science and technology to the problem of modeling adsorption dynamics in building zones. We begin by considering the adsorption dynamics of a single contaminant species α in a well-mixed building zone containing a volume of air with mass m_Z and a quantity of adsorbent material with mass m_S. The (average) concentration of the contaminant species in the zone air will be identified as ${}^{\alpha}C_Z$ and the average concentration in the adsorbent as ${}^{\alpha}C_S$, both expressed in terms of mass fraction (i.e., (mass α)/(mass air) and (mass α)/(mass adsorbent) respectively).

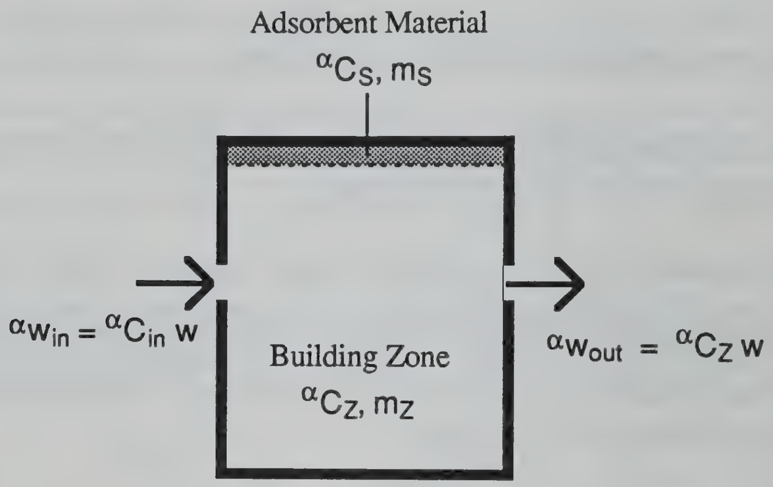
Adsorbent Material
${}^{\alpha}C_S, m_S$
${}^{\alpha}w_{in} = {}^{\alpha}C_{in}\, w$
Building Zone
${}^{\alpha}C_Z, m_Z$
${}^{\alpha}w_{out} = {}^{\alpha}C_Z\, w$

Figure 3.1 Zone plus adsorbent control volume.

If the mass flow rate of air into the zone is w and the species concentration flowing into the zone is ${}^{\alpha}C_{in}$, then the mass flow rates of species α into the zone and out of the zone, ${}^{\alpha}w_{in}$ and ${}^{\alpha}w_{out}$, are simply equal to the product of the respective concentrations and the air mass flow rate as:

$$ {}^{\alpha}w_{in} = {}^{\alpha}C_{in}\, w \tag{3.1}$$

$$ {}^{\alpha}w_{out} = {}^{\alpha}C_Z\, w \tag{3.2}$$

In an analogous manner we may describe the species mass flow rate by adsorption and desorption transport between the room and the adsorbent material in terms of discrete or lumped species mass flow rates, ${}^{\alpha}w_{ads}$ and ${}^{\alpha}w_{des}$, that will, in general, depend on the zone and adsorbent concentrations as well as the physical characteristics of the adsorbate species α, adsorbent material, and the detailed nature of the airflow in the room:

$$^{\alpha}w_{ads} = f_{ads}(^{\alpha}C_Z, {}^{\alpha}C_S, \ldots) \tag{3.3}$$

$$^{\alpha}w_{des} = f_{des}(^{\alpha}C_Z, {}^{\alpha}C_S, \ldots) \tag{3.4}$$

Isolating the control volume surrounding the adsorbent from the control volume surrounding the zone air, the adsorption and desorption mass flow rates may be diagrammatically represented as shown in Figure 3.2.

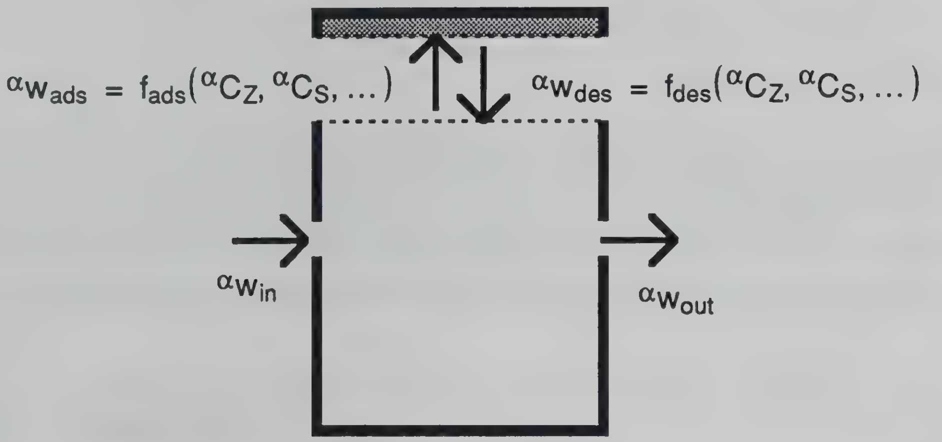

$^{\alpha}w_{ads} = f_{ads}(^{\alpha}C_Z, {}^{\alpha}C_S, \ldots)$
$^{\alpha}w_{des} = f_{des}(^{\alpha}C_Z, {}^{\alpha}C_S, \ldots)$
$^{\alpha}w_{in}$
$^{\alpha}w_{out}$

Fig. 3.2 Zone control volume and adsorbent control volume.

Limiting consideration for the moment to completely reversible adsorption (i.e., allowing no irreversible destruction or transformation of the adsorbate species α in the adsorbent material or in the building zone) we may immediately write species mass balance relations for the adsorbent material, the building zone, and the systems as a whole as:

Building Zone Mass Balance

$$(^{\alpha}w_{out} - {}^{\alpha}w_{in}) + (^{\alpha}w_{ads} - {}^{\alpha}w_{des}) + m_Z\frac{d^{\alpha}C_Z}{dt} = {}^{\alpha}G_Z \tag{3.5}$$

Adsorbent Material Mass Balance

$$(^{\alpha}w_{des} - {}^{\alpha}w_{ads}) + m_S\frac{d^{\alpha}C_S}{dt} = {}^{\alpha}G_S \tag{3.6}$$

Building Zone and Adsorbent Material Mass Balance

$$(^{\alpha}w_{out} - {}^{\alpha}w_{in}) + m_Z\frac{d^{\alpha}C_Z}{dt} + m_S\frac{d^{\alpha}C_S}{dt} = {}^{\alpha}G_Z + {}^{\alpha}G_S \tag{3.7}$$

where we admit the possibility of generation of the contaminant species α in both the building zone, $^{\alpha}G_Z$, and the adsorbent material, $^{\alpha}G_S$.

Irreversible destruction or transformation of the contaminant species in the adsorbent or in the building zone may be introduced by introducing appropriate transformation kinetics expressions for either or both of the generation terms above, ${}^{\alpha}G_Z$ and ${}^{\alpha}G_S$. Thus, for example, if the analyst wishes to model linear destruction kinetics in the adsorbent ${}^{\alpha}G_S$ would be replaced by an expression of the form ${}^{\alpha}G_S = (-m_S\kappa_S)\,{}^{\alpha}C_S$, where κ_S is the first order rate constant associated with the destruction. To allow a focused consideration of (reversible) physical adsorption irreversible transformation will not be considered further.

Equilibrium Adsorption

To provide some insight into the dynamics of this coupled system it is useful to consider a limiting case where the adsorbed species concentration remains in equilibrium with the zone concentration (i.e., the species mass transport rate by adsorption or desorption is practically instantaneous). More specifically, if the equilibrium relationship is described by the Linear Model:

$$ {}^{\alpha}C_S = K_P\,{}^{\alpha}C_Z \qquad \textit{Linear Model} \qquad (3.8a) $$

or:

$$ \frac{d\,{}^{\alpha}C_S}{dt} = K_P\frac{d\,{}^{\alpha}C_Z}{dt} \qquad (3.8b) $$

the mass balance for the system as a whole, Equation 3.7 with Equations 3.1 and 3.2, simplifies to:

$$ \boxed{w\,{}^{\alpha}C_Z + (m_Z + K_P m_S)\frac{d\,{}^{\alpha}C_Z}{dt} = {}^{\alpha}E} \qquad \textit{Linear Equilibrium Adsorption} \qquad (3.9a) $$

$$ {}^{\alpha}E = \left({}^{\alpha}G_Z + {}^{\alpha}G_S + w\,{}^{\alpha}C_{in}\right) \qquad (3.9b) $$

where all forcing terms have been collected on the right hand side to define the system *excitation* , ${}^{\alpha}E$.

Alternatively, if the equilibrium relationship is described by the Langmuir Model:

$$ {}^{\alpha}C_S = \frac{{}^{\alpha}C_{So}K_L\,{}^{\alpha}C_Z}{1 + K_L\,{}^{\alpha}C_Z} \qquad \textit{Langmuir Model} \qquad (3.10a) $$

or:

$$\frac{d\,{}^{\alpha}C_S}{dt} = \left(\frac{{}^{\alpha}C_{So}K_L}{(1 + K_L{}^{\alpha}C_Z)^2}\right)\frac{d\,{}^{\alpha}C_Z}{dt} \qquad (3.10b)$$

the mass balance for the system as a whole simplifies to:

$$\boxed{w\,{}^{\alpha}C_Z + \left(m_Z + \left(\frac{{}^{\alpha}C_{So}K_L}{(1 + K_L{}^{\alpha}C_Z)^2}\right)m_S\right)\frac{d\,{}^{\alpha}C_Z}{dt} = {}^{\alpha}E} \quad \textit{Langmuir Equilib.Adsorption} \qquad (3.11)$$

For both cases the adsorbent acts to increase the participating mass of the building zone from that of the mass of the air in the zone, m_Z, to this quantity plus the mass of the adsorbent, m_S, scaled by a factor. For Linear equilibrium, the effective participating mass is:

$$m_{effective} = m_Z + K_P m_S \qquad \textit{Linear Equilibrium Adsorption} \qquad (3.12)$$

For the Langmuir Model the scaling factor includes a nonlinear dependency on the zone concentration:

$$m_{effective} = m_Z + \left(\frac{{}^{\alpha}C_{So}K_L}{(1 + K_L{}^{\alpha}C_Z)^2}\right)m_S \qquad \textit{Langmuir Equilibrium Adsorption} \quad (3.13)$$

but for situations where the zone concentration does not vary greatly, this factor will remain reasonably constant as well. Furthermore, for those situations where the zone concentration is small enough so that the $K_L{}^{\alpha}C_Z$ term in the denominator may be neglected then this factor should be expected to equal the partition coefficient of the Linear Model (as discussed earlier).

For a single well-mixed zone under conditions of constant flow the system time constant, τ, (or its inverse, the nominal air change rate);

$$\tau \equiv (m_Z/w) \quad ; \quad w = \text{constant} \qquad \textit{Well-mixed Zone} \qquad (3.14)$$

provides a concise and convenient measure of the systems dispersal dynamics. For a well-mixed zone under conditions of constant flow with linear equilibrium adsorption dynamics added from Equation 3.9 it is seen that the system time constant, τ, becomes:

$$\tau \equiv (m_{effective}/w) \quad ; \quad w = \text{constant} \qquad \textit{Well-mixed Zone with Equilib. Adsorption} \qquad (3.15)$$

/// **Example Application: Equilibrium Adsorption in a Room**

To fix these ideas and to evaluate the potential significance of the participating mass offered by real adsorbents in building construction it is useful, at this point, to consider a practical example. To this end, consider a room 5 x 8 m in plan with a 3 m floor to ceiling height, 25 mm thick nylon carpeting, and 13 mm thick gypsum board walls and ceiling, as sketched below.

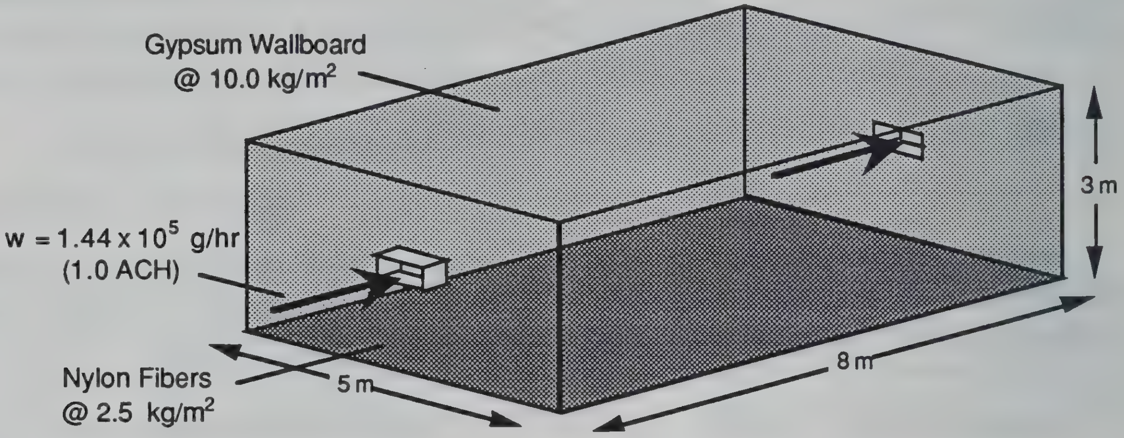

The approximate weight of the gypsum board may be estimated at 10 kg/m^2 and that of the nylon fibers in the carpeting at 2.5 kg/m^2 thus, given the room geometry, the total mass of gypsum board is approximately 7.8 x 10^5 g or:

$$m_{gyp} \approx 7.8 \times 10^5 \text{ g}$$

and for the nylon fibers in the carpet approximately 1.00 x 10^5 g or:

$$m_{nylon} \approx 1.0 \times 10^5 \text{ g}$$

At standard conditions of temperature and pressure the density of the air in the room is very nearly 1.2 kg/m^3 thus the mass of air in the room is some 1.44 x 10^5 g or:

$$m_Z \approx 1.44 \times 10^5 \text{ g}$$

Researchers at both the Oak Ridge National Laboratories and the National Institute of Standards and Technology report partition coefficients for the formaldehyde (HCHO)–gypsum wallboard system at 23°C and 50% RH to be approximately 5.5 g-air/g-gypboard[4] [12, 18, 19]. If we assume equilibrium adsorption conditions prevail, then, for this measured partition coefficient and the representative room considered here, the gypboard may be expected to contribute a participating mass of:

---

[4] ORNL researchers reported a "CH$_2$O capacity" of 23 (m^3-air/m^2-gypboard) while Silberstein at NIST measured capacities of 46 and 47 (m^3-air/m^2-gypboard). Both measurements were based on mixed units of HCHO surface concentration expressed in units of (mg-HCHO/m^2-gypboard) and air concentration expressed in units of (mg-HCHO/m^3-air), but ORNL considered exposure of both sides of gypsum board specimens while Silberstein considered exposure on only a single side. When expressed in mass fraction units these effective

$$
\begin{aligned}
{}^{\text{HCHO-gypboard}}K_P\, m_{gyp} &= 5.52\ (\text{g-air/g-gyp}) \times 7.8 \times 10^5\ (\text{g-gyp}) \\
&= 43 \times 10^5\ (\text{g-air})
\end{aligned}
$$

that effectively increases the room air mass, m_Z, by a factor of 31. This effective increase in room air mass would result in an equal increase in the apparent time constant of the well-mixed zone, for conditions of constant airflow. Thus, for example, for a well-mixed zone without adsorption having a time constant of 1 hour (i.e., an air exchange rate of 1 air change per hour) the gypboard would effectively alter the time constant for HCHO dispersal to 31 hours.

In another study [1] partition coefficients for nylon, wool, and glass fibers are reported for some nine different aromatic and chlorinated hydrocarbons, designated simply as H-C-Cl here. For nylon fibers these partition coefficients range from 2.4 to 16.8 x 10^{-4} g-air/g-nylon fibers[5]. If, again, we assume equilibrium adsorption conditions prevail, then, the nylon fibers in the carpet of the representative room being considered may be expected to contribute a participating mass of:

$$
\begin{aligned}
{}^{\text{H-C-Cl-nylon}}K_P\, m_{nylon} &= (2.4\ \text{ to }\ 16.8) \times 10^{-4}(\text{g-air/g-nylon}) \times 1.0 \times 10^5\ (\text{g-nylon}) \\
&= (2.4\ \text{ to }\ 16.8) \times 10\ (\text{g-air})
\end{aligned}
$$

In this case the room air mass would be effectively increased only slightly by 0.01 to 0.10%. ///

These simple calculations based on the equilibrium adsorption assumption indicate that adsorption can dramatically alter the dynamics of contaminant dispersal in rooms when the product of the adsorbent mass and its partition coefficient are significant. Some first experimental studies of adsorption in rooms support this conclusion [12, 18, 19].

Boundary Layer Diffusion Controlled Adsorption

In general, adsorption mass transport rates are determined by the individual transport rates of the diffusion processes and the surface adsorption kinetics that together account for the

---

partition factors are, therefore, equivalent. Conversion from these units to the mass fraction units of (g-air/g-gypboard) was based on an air density of 1.2 kg/m^3, gypboard bulk density of 769 kg/m^3, and a gypboard thickness of 13 mm.

[5] The reported partition coefficient of 0.2 to 1.4 (cm^3-air/g-nylon) were converted to the mass fraction units of (g-air/g-gypboard) based on an air density of 1.2 kg/m^3.

multiple steps in the overall adsorption transport process. Throughout the adsorption literature, however, it is emphasized that adsorption dynamics, in most practical situations, is invariably controlled by diffusion transport - the adsorption kinetics step is practically instantaneous - although exceptions to this general rule exist[6] [8]. With this in mind, we will consider models for room adsorption dynamics that account for external film diffusion based on the assumptions that:

> a) equilibrium exists at the solid-gas interface at all times as defined by one of the equilibrium isotherms considered above (i.e., the kinetics of adsorption is practically instantaneous) and
>
> b) the system remains practically isothermal (i.e., the rate of heat generation due to adsorption is negligibly small and the heat transfer processes are sufficiently large to maintain isothermal conditions).

Models for room adsorption dynamics that account for macropore diffusion and micropore diffusion will be considered in subsequent studies.

Adsorption mass transport rates from the room air to solid (i.e., nonporous) adsorbents with reasonably smooth surfaces may be expected to be controlled by the rate at which a contaminant species diffuses from the bulk phase to the surface of the adsorbent. The diffusion mass transport rate will, in general, depend on the details of the contaminant concentration and velocity fields in the room. Details that are both difficult to measure and to determine analytically (e.g., by computational fluid dynamics) and, consequently, details that will not normally be known nor easily determined. For wall surfaces and other larger flat surfaces in rooms it is likely that any flow that exists will be directed more or less parallel to these surfaces forming a boundary layer over the surface of interest. Therefore, to obtain estimates of diffusion mass transport for these surfaces, we may reasonably apply some key results from boundary layer theory.

The adsorbent surface may be thought to be separated from the room air by a *film* of air (i.e., the boundary layer) over which the contaminant concentration varies from a near-surface, air-phase concentration, ${}^{\alpha}C_Z^*$, to the bulk air-phase concentration in the zone, ${}^{\alpha}C_Z$, as illustrated in Figure 3.3. (Anticipating the formulation, we will assume that this near-surface, air phase concentration will remain in equillibrium with the adsorbed-phase concentration and, hence, use the "*" notation indicating an equilibrium concentration.)

---

[6] Ethier and Kamm consider cases (e.g. the adsorption of large molecules on surfaces of very small pores) where adsorption kinetics controls the overall adsorption dynamics.

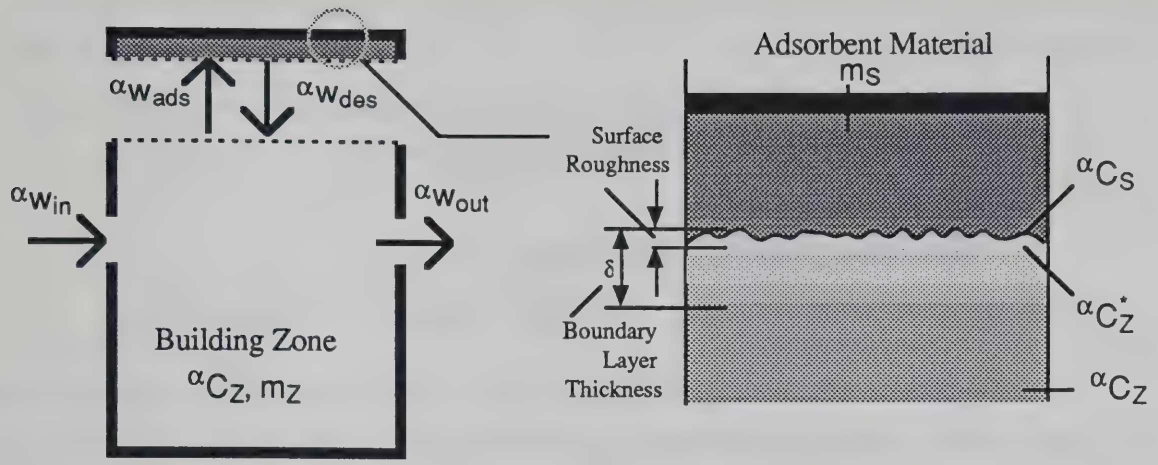

Fig 3.3 Boundary layer diffusion controlled adsorption.

If mass transport to the adsorbent is due only to *film* diffusion (e.g., there is no bulk flow of contaminant through the adsorbent due to pressure gradients within or across the adsorbent) and the air-phase concentrations are not varying too rapidly, then the net mass transport rate from the bulk phase to the surface, ${}^{\alpha}w_S$, may be approximated using steady-state mass transfer relations from boundary layer theory[7] [21] of the general form:

$$ {}^{\alpha}w_S \equiv \left({}^{\alpha}w_{ads} - {}^{\alpha}w_{des}\right) = \overline{h_m}\,\rho\,A_S\left({}^{\alpha}C_Z - {}^{\alpha}C_Z^{*}\right) \qquad (3.16) $$

where;

$\overline{h_m}$ is the average *film* mass transfer coefficient acting over the adsorbent surface (length/(time)

ρ is the *film* density of air, the average of the bulk and surface densities

A_S is the projected surface area of the adsorbent

A dimensionless form of the average *film* mass transport coefficient, the average Sherwood number, $\overline{Sh_L}$, may be correlated with the surface flow Reynolds number, Re_L, and the air phase Schmidt number, Sc, as:

$$ \overline{Sh_L} \equiv \frac{\overline{h_m}\,L}{{}^{\alpha\text{-air}}D} = 0.664\,Re_L^{1/2}Sc^{1/3} \quad ; \quad \text{for} \quad Re_L < 500{,}000 \qquad (3.17a) $$

$$ \overline{Sh_L} \equiv \frac{\overline{h_m}\,L}{{}^{\alpha\text{-air}}D} = 0.037\,Re_L^{4/5}Sc^{1/3} \quad ; \quad \text{for} \quad Re_L > 500{,}000 \quad ; \quad Sc \approx 1.0 \qquad (3.17b) $$

where;

---

[7] The correlations used here are based on steady conditions of surface and bulk concentrations, stationary flow conditions parallel to the wall, and diffusion due to concentration gradients only, ignoring the so-called *blowing effect* (which must be expected to be small for mass fraction concentrations less than 0.2).

$Re_L = \frac{UL}{\nu}$

U is the mean fluid velocity (parallel to the surface) outside of the boundary layer

L is the length of the surface in the direction of the flow

$Sc = \frac{\nu}{{}_{\alpha\text{-air}}D}$

ν is the kinematic viscosity of the air phase

${}_{\alpha\text{-air}}D$ is the molecular diffusivity of the binary α-air system being considered

For many gases in air the molecular diffusivity is practically constant with concentration (although it varies directly with temperature and inversely with pressure) with values, at room temperature and atmospheric pressure, ranging from 10^{-5} to 10^{-4} m^2/s and the Schmidt number is typically close to 1.0 (e.g., 0.2 to 2.0). For a Schmidt number equal to 1.0 the average Sherwood number varies as plotted below.

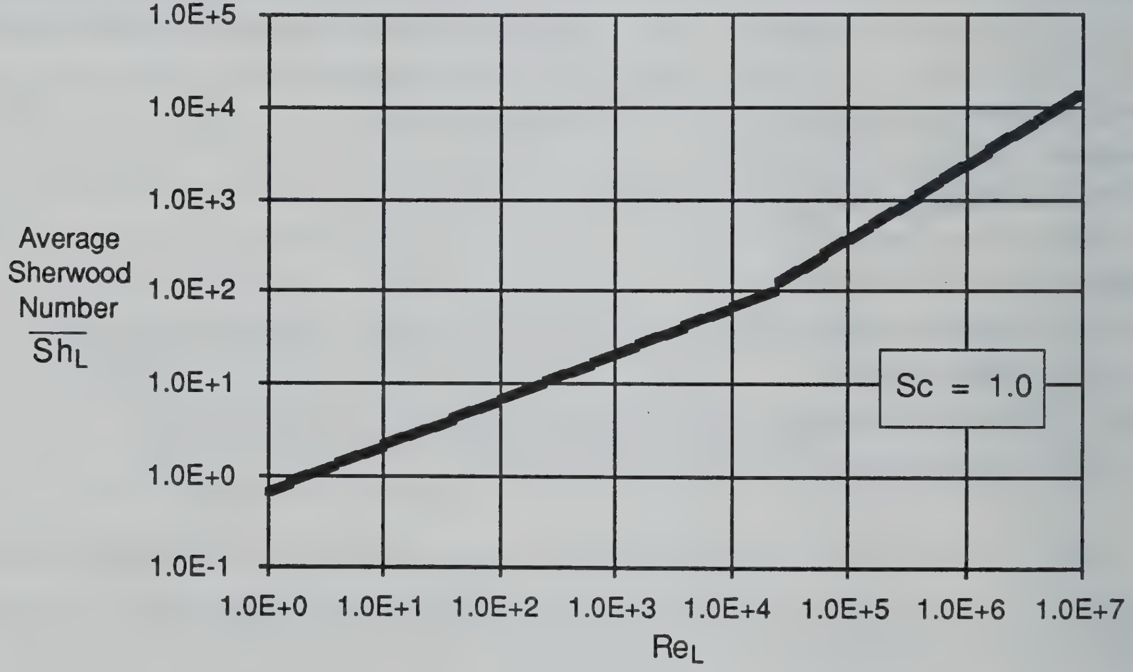

At relatively low flow conditions the Sherwood number approaches 1.0 as molecular diffusion, rather than convective transport, becomes dominant. At very low flow conditions, however, the average Sherwood number, from these correlations, goes to zero when, in fact, molecular diffusion should remain dominant, therefore, for our considerations here we will assume:

$$\overline{Sh_L} \equiv \frac{\overline{h_m} L}{{}_{\alpha\text{-air}}D} \cong 1.0 \quad ; \quad \text{for } Re_L \leq 5 \quad ; \quad Sc \approx 1.0 \tag{3.17c}$$

With the expression for film diffusion transport, Equation 3.16, in hand we may formulate equations that describe the system adsorption dynamics by first demanding equilibrium at the adsorbent surface:

$$ {}^{\alpha}C_S = K_P {}^{\alpha}C_Z^{*} \qquad \textit{Linear Model} \qquad (3.18) $$

or

$$ {}^{\alpha}C_S = \frac{{}^{\alpha}C_{So} K_L {}^{\alpha}C_Z^{*}}{1 + K_L {}^{\alpha}C_Z^{*}} \qquad \textit{Langmuir Model} \qquad (3.19) $$

and then substituting these equations and Equations 3.1, 3.2, and 3.16, into the basic mass balance relations for the system, Equations 3.5 and 3.6, to obtain, after simplification:

a) for the Linear Model:

$$ \left({}^{\alpha}C_Z w - {}^{\alpha}C_{in} w\right) + \overline{h}_m \rho A_S \left({}^{\alpha}C_Z - \frac{{}^{\alpha}C_S}{K_P}\right) + m_Z \frac{d{}^{\alpha}C_Z}{dt} = {}^{\alpha}G_Z \qquad (3.20a) $$

$$ -\overline{h}_m \rho A_S \left({}^{\alpha}C_Z - \frac{{}^{\alpha}C_S}{K_P}\right) + m_S \frac{d{}^{\alpha}C_S}{dt} = {}^{\alpha}G_S \qquad (3.20b) $$

or, alternatively:

Linear Boundary Layer Diffusion Controlled Adsorption

$$ \boxed{ \begin{bmatrix} w + \overline{h}_m \rho A_S & -\dfrac{\overline{h}_m \rho A_S}{K_P} \\ -\overline{h}_m \rho A_S & \dfrac{\overline{h}_m \rho A_S}{K_P} \end{bmatrix} \begin{Bmatrix} {}^{\alpha}C_Z \\ {}^{\alpha}C_S \end{Bmatrix} + \begin{bmatrix} m_Z & 0 \\ 0 & m_S \end{bmatrix} \begin{Bmatrix} \dfrac{d{}^{\alpha}C_Z}{dt} \\ \dfrac{d{}^{\alpha}C_S}{dt} \end{Bmatrix} = \{{}^{\alpha}\mathbf{E}\} } \qquad (3.20c) $$

where, we have collected all forcing terms on the right hand side as the system *excitation vector*, $\{{}^{\alpha}\mathbf{E}\}$:

$$ \{{}^{\alpha}\mathbf{E}\} = \begin{Bmatrix} {}^{\alpha}G_Z + {}^{\alpha}C_{in} w \\ {}^{\alpha}G_S \end{Bmatrix} \qquad (3.20d) $$

b) for the Langmuir Model:

$$ \left({}^{\alpha}C_Z w - {}^{\alpha}C_{in} w\right) + \overline{h}_m \rho A_S \left({}^{\alpha}C_Z - \frac{{}^{\alpha}C_S}{K_L\left({}^{\alpha}C_{SO} - {}^{\alpha}C_S\right)}\right) + m_Z \frac{d{}^{\alpha}C_Z}{dt} = {}^{\alpha}G_Z \qquad (3.21a) $$

$$-\overline{h_m}\,\rho\,A_S\left({}^{\alpha}C_Z-\frac{{}^{\alpha}C_S}{K_L\left({}^{\alpha}C_{SO}-{}^{\alpha}C_S\right)}\right)+m_S\frac{d^{\alpha}C_S}{dt}={}^{\alpha}G_S \qquad (3.21b)$$

or, alternatively:

Langmuir Boundary Layer Diffusion Controlled Adsorption

$$\boxed{\begin{bmatrix} w+\overline{h_m}\,\rho\,A_S & -\dfrac{\overline{h_m}\,\rho\,A_S}{K_L\left({}^{\alpha}C_{SO}-{}^{\alpha}C_S\right)} \\ -\overline{h_m}\,\rho\,A_S & \dfrac{\overline{h_m}\,\rho\,A_S}{K_L\left({}^{\alpha}C_{SO}-{}^{\alpha}C_S\right)} \end{bmatrix}\begin{Bmatrix} {}^{\alpha}C_Z \\ {}^{\alpha}C_S \end{Bmatrix}+\begin{bmatrix} m_Z & 0 \\ 0 & m_S \end{bmatrix}\begin{Bmatrix} \dfrac{d^{\alpha}C_Z}{dt} \\ \dfrac{d^{\alpha}C_S}{dt} \end{Bmatrix}=\{{}^{\alpha}E\}} \qquad (3.21c)$$

(The Langmuir Model Equations 3.21 are valid only up to the condition of complete coverage of the surface (i.e., $(C_{SO}-C_S)>0$) at which point Equations 3.21 become singular.)

The Linear Model and Langmuir Model variants of the system adsorption dynamics equations considered so far may be represented in concise notation as:

$$[{}^{\alpha}\mathbf{W}]\{{}^{\alpha}\mathbf{C}\}+[{}^{\alpha}\mathbf{M}]\frac{d\{{}^{\alpha}\mathbf{C}\}}{dt}=\{{}^{\alpha}\mathbf{E}\} \qquad (3.22a)$$

where:

a) for *Equilibrium Adsorption*:

$$\{{}^{\alpha}\mathbf{C}\}\equiv{}^{\alpha}C_Z \qquad (3.22b)$$

$$[{}^{\alpha}\mathbf{W}]=w \qquad (3.22c)$$

$$[{}^{\alpha}\mathbf{M}]=m_Z+K_P m_S \qquad \textit{Linear Model} \qquad (3.22d)$$

or

$$[{}^{\alpha}\mathbf{M}]=m_Z+\left(\frac{{}^{\alpha}C_{So}K_L}{\left(1+K_L{}^{\alpha}C_Z\right)^2}\right)m_S \qquad \textit{Langmuir Model} \qquad (3.22e)$$

b) for *Boundary Layer Diffusion Controlled Adsorption*

$$\{{}^{\alpha}\mathbf{C}\}\equiv\begin{Bmatrix} {}^{\alpha}C_Z \\ {}^{\alpha}C_S \end{Bmatrix} \qquad (3.22f)$$

$$[{}^{\alpha}\mathbf{M}] = \begin{bmatrix} m_Z & 0 \\ 0 & m_S \end{bmatrix} \tag{3.22g}$$

$$[{}^{\alpha}\mathbf{W}] = \begin{bmatrix} w+\overline{h_m}\,\rho\,A_S & -\dfrac{\overline{h_m}\,\rho\,A_S}{K_P} \\ -\overline{h_m}\,\rho\,A_S & \dfrac{\overline{h_m}\,\rho\,A_S}{K_P} \end{bmatrix} \qquad \textit{Linear Model} \tag{3.22h}$$

or

$$[{}^{\alpha}\mathbf{W}] = \begin{bmatrix} w+\overline{h_m}\,\rho\,A_S & -\dfrac{\overline{h_m}\,\rho\,A_S}{K_L(C_{SO}-C_S)} \\ -\overline{h_m}\,\rho\,A_S & \dfrac{\overline{h_m}\,\rho\,A_S}{K_L(C_{SO}-C_S)} \end{bmatrix} \qquad \textit{Langmuir Model} \tag{3.22i}$$

Note that the Langmuir Model introduces nonlinearity in the *mass matrix*, $[{}^{\alpha}\mathbf{M}]$, of the Equilibrium Adsorption (EA) Model (i.e., with respect to zone concentration, ${}^{\alpha}C_Z$) and in the *transport matrix*, $[{}^{\alpha}\mathbf{W}]$, of the Boundary Layer Diffusion Controlled Adsorption (BLDC) Model (i.e., with respect to zone concentration, ${}^{\alpha}C_S$). Similar models can be directly developed for the BET and Freundlich equilibrium adsorption isotherms. If developed, these models will also reveal nonlinearities in the mass matrix for the EA Model and the transport matrix in the BLDC Model although the forms or nonlinearity will be different from those above. These alternate models may be considered in subsequent studies.

The essential dynamic character of the (scalar) EA Model is contained in the system time constant, τ, or equivalently the system eigenvalue, $\lambda = 1/\tau$, which is equal to $\lambda = [{}^{\alpha}\mathbf{M}]^{-1}[{}^{\alpha}\mathbf{W}] = (w/m_{\text{effective}})$. Analogously, the essential dynamic character of the coupled BLDC Model equations is contained in the coupled system eigenvalues that satisfy the characteristic equation of the system:

$$\det\left|\,[{}^{\alpha}\mathbf{M}]^{-1}[{}^{\alpha}\mathbf{W}] - \lambda[\mathrm{I}]\,\right| = 0 \tag{3.23}$$

where, for the Langmuir Model this eigenvalue problem would be evaluated at each specific state of the adsorbent concentration, ${}^{\alpha}C_S$, given the nonlinearity of the mass transport matrix in this case. In general this eigenvalue problem has two solutions, $\{\lambda_1, \lambda_2\}$; the inverses of the system time constants, $\{\tau_1, \tau_2\}$:

$$[\Lambda] \equiv \begin{bmatrix} \lambda_1 & 0 \\ 0 & \lambda_2 \end{bmatrix} = \begin{bmatrix} 1/\tau_1 & 0 \\ 0 & 1/\tau_2 \end{bmatrix} \tag{3.24}$$

If we substitute the Linear Model, Equations 3.20, into 3.23 we obtain of the familiar form:

$$a\lambda^2 + b\lambda + c = 0 \tag{3.25a}$$

with:

$$a = 1.0 \tag{3.25b}$$

$$b = -\frac{(\overline{{}^{\alpha}h_m}\rho A_S + w)K_P m_S + \overline{{}^{\alpha}h_m}\rho A_S m_Z}{K_P m_S m_Z} \tag{3.25c}$$

$$c = \frac{\overline{{}^{\alpha}h_m}\rho A_S w}{K_P m_S m_Z} \tag{3.25d}$$

The two solutions of this quadratic relation, $\lambda = \left(-b \pm \sqrt{b^2 - 4ac}\right)\big/2a$, for the variables here, yield the two eigenvalues of the Linear Model:

$$\lambda = \frac{(\overline{{}^{\alpha}h_m}\rho A_S + w)K_P m_S + \overline{{}^{\alpha}h_m}\rho A_S m_Z}{2K_P m_S m_Z} \pm \frac{1}{2}\sqrt{\left(\frac{(\overline{{}^{\alpha}h_m}\rho A_S + w)K_P m_S + \overline{{}^{\alpha}h_m}\rho A_S m_Z}{K_P m_S m_Z}\right)^2 - 4\frac{\overline{{}^{\alpha}h_m}\rho A_S w}{K_P m_S m_Z}} \tag{3.26}$$

It is interesting to consider three limiting cases:

a) *No Diffusion:* When diffusion from the building zone to the adsorbent surface drops to zero, $\overline{{}^{\alpha}h_m}\rho A_S = 0$, the system eigenvalues correspond to the eigenvalue of the well-mixed zone without adsorption, by direct substitution in Equation 3.26, as expected:

$$\begin{bmatrix} \lambda_1 & 0 \\ 0 & \lambda_2 \end{bmatrix} = \begin{bmatrix} (w/m_Z) & 0 \\ 0 & 0 \end{bmatrix} \quad ; \text{ when: } \overline{{}^{\alpha}h_m}\rho A_S = 0 \tag{3.27}$$

b) *No Infiltration:* When the infiltration into the zone drops to zero, $w = 0$, the system eigenvalues become, by direct substitution in Equation 3.26:

$$\begin{bmatrix} \lambda_1 & 0 \\ 0 & \lambda_2 \end{bmatrix} = \begin{bmatrix} \left(\frac{\overline{{}^{\alpha}h_m}\rho A_S(K_P m_S + m_Z)}{K_P m_S m_Z}\right) & 0 \\ 0 & 0 \end{bmatrix} \quad ; \text{ when: } w = 0 \tag{3.28}$$

Note that as the first eigenvalue increases linearly with the diffusion mass transfer rate, $\overline{\alpha h_m \rho A_S}$, with the result that the system time constant, $\tau_1 = 1/\lambda_1$, approaches zero as the mass transfer rate increases.

c) *Equilibrium Adsorption:* If the rate of diffusion, $\overline{\alpha h_m \rho A_S}$, is large relative to the infiltration mass flow rate, w, then the system eigenvalues approach those corresponding to the Linear Equilibrium Adsorption Model (i.e., from Equations 3.12 and 3.15):

$$\begin{bmatrix} \lambda_1 & 0 \\ 0 & \lambda_2 \end{bmatrix} \rightarrow \begin{bmatrix} \left(\dfrac{\overline{\alpha h_m \rho A_S}(K_P m_S + m_Z)}{K_P m_S m_Z}\right) & 0 \\ 0 & \dfrac{w}{K_P m_S + m_Z} \end{bmatrix} ; \text{ when: } \overline{\alpha h_m \rho A_S} >> w \qquad (3.29)$$

Again the first eigenvalue increases linearly with diffusion mass transfer rate.

The proof of Equation 3.29 is rather indirect. The quantities $\left(\overline{\alpha h_m \rho A_S} + w\right)$ in Equation 3.26 may be replaced by $\overline{\alpha h_m \rho A_S}$ for $\overline{\alpha h_m \rho A_S} >> w$ and the resulting equation simplified to yield:

$$\lambda = \frac{\overline{\alpha h_m \rho A_S}\,(K_P m_S + m_Z)}{2K_P m_S m_Z} \pm \frac{\overline{\alpha h_m \rho A_S}\,(K_P m_S + m_Z)}{2K_P m_S m_Z}\sqrt{1 - 4\frac{w K_P m_S m_Z}{\overline{\alpha h_m \rho A_S}\,(K_P m_S + m_Z)^2}} \qquad (3.30)$$

By forming a Taylor's expansion of the square root term:

$$\sqrt{1 - 4\frac{w K_P m_S m_Z}{\overline{\alpha h_m \rho A_S}\,(K_P m_S + m_Z)^2}}$$

$$= 1 - 2\frac{w K_P m_S m_Z}{\overline{\alpha h_m \rho A_S}\,(K_P m_S + m_Z)^2} - \left(\frac{1}{2}\right)\left(\frac{w K_P m_S m_Z}{\overline{\alpha h_m \rho A_S}\,(K_P m_S + m_Z)^2}\right)^2 - \ldots$$

$$\approx 1 - 2\frac{w K_P m_S m_Z}{\overline{\alpha h_m \rho A_S}\,(K_P m_S + m_Z)^2} ; \text{ when: } \overline{\alpha h_m \rho A_S} >> w \qquad (3.31)$$

substituting this result into Equation 3.30 and simplifying we obtain the results above.

/// **Example Application: Boundary Layer Diffusion Controlled Adsorption in a Room**

To fix these ideas and to evaluate the significance of the diffusion transport reconsider the room studied earlier using the Adsorption Equilibrium Model now applying, instead, the BLDC Model. This time we will limit consideration to the adsorption of formaldehyde, HCHO, by gypsum board having the partition coefficient considered earlier, $K_P = 5.5$ g-air/g-nylon fibers. The area of the adsorbent in this case is $A_S = 118\ \text{m}^2$. Assuming air flows uniformly from the inlet to the outlet, a reasonable estimate of the effective length of the adsorbent surface would be $L = 8$ m and an estimate of the free stream velocity of the air flow would be $U = 8$ m/hr $= 0.00222$ m/s (i.e., given the flow rate of 1 air change per hour, the volumetric flow divided by the room cross sectional area). Thus the effective Reynolds number would be (with the kinematic viscosity of the air of $\nu \approx 1.5 \times 10^{-5}\ \text{m}^2/\text{s}$):

$$Re_L = \frac{UL}{\nu} = \frac{(0.0022)(8)}{1.5 \times 10^{-5}} = 1{,}173$$

For a Scmidt number of 1.0 we, thus, obtain the average Sherwood number for this problem, from Equation 3.17a, as:

$$\overline{Sh_L} = 0.664\, Re_L^{1/2} Sc^{1/3} = 0.664(1173)^{1/2}(1.0)^{1/3} = 22.7$$

For a representative gas diffusivity of ${}^{\text{HCHO-air}}D = 1.4 \times 10^{-5}\ \text{m}^2/\text{s}$ we obtain an estimate of the film diffusion mass transfer coefficient from Equations 3.17 as:

$$\overline{h_m} \approx \overline{Sh_L}\left(\frac{{}^{\text{HCHO-air}}D}{L}\right) = 22.7\left(\frac{1.4 \times 10^{-5}}{8}\right) = 3.97 \times 10^{-5}\ \text{m/s}$$

With these values in hand, an infiltration rate of $w = 40$ g/s (i.e., based on 1.0 air change per hour and an air density of 1,200 g/m^3), and the zone and adsorbent masses computed earlier:

$$m_Z = 1.44 \times 10^5\ \text{g} \ ; \ m_S = 7.8 \times 10^5\ \text{g}$$

we may apply Equations 3.25 to compute the eigenvalues for the gypboard/room system:

$$\lambda_1 = 3.17 \times 10^{-4}\ \text{s}^{-1} = 1.14\ \text{hr}^{-1} \ \underline{\text{or}}\ \tau_1 = 0.876\ \text{hr}$$

$$\lambda_2 = 1.15 \times 10^{-6}\ \text{s}^{-1} = 4.14 \times 10^{-3}\ \text{hr}^{-1} \ \underline{\text{or}}\ \tau_2 = 242\ \text{hr}$$

revealing a *bimodal* response characterized by a very long time constant of 242 hr (i.e., 10.1 days) and a quick response somewhat smaller than the nominal system time constant without adsorption (i.e., $(m_Z/w) = 1.0$ hr). This sort of response behavior has, in fact, been observed in experimental studies [12, 18, 19]; the results of these studies will be considered subsequently.

The response of this system, and other systems governed by the BLDC Model, is particularly sensitive to boundary layer diffusion rate as characterized by the average Sherwood number. Plotted below, for this example case, is the variation of the system time constants for a variation of average Sherwood number:

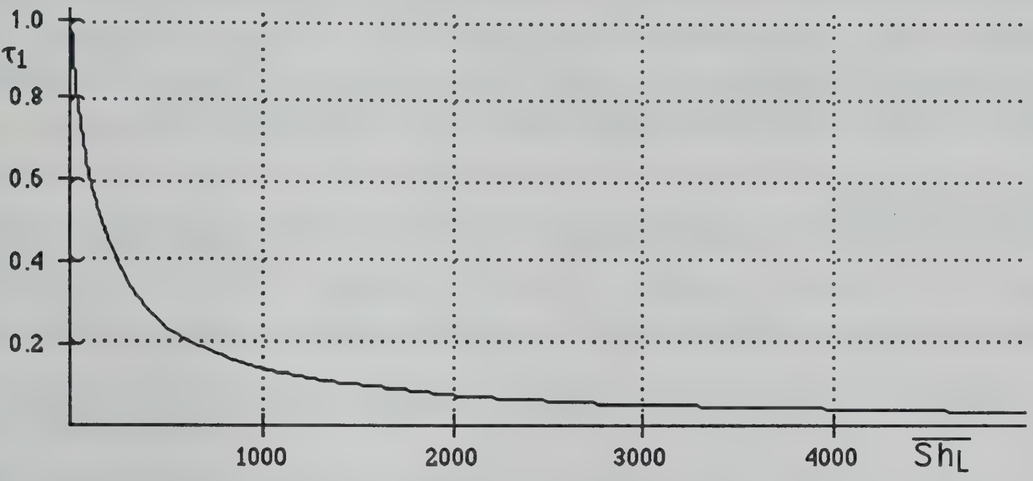

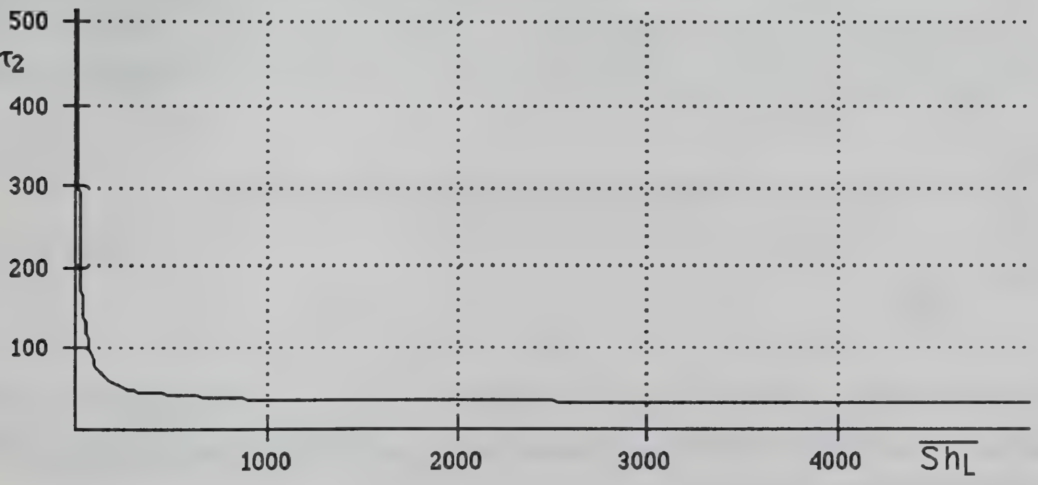

It is seen that the first time constant, τ_1, diminishes from 1.0 hr to zero as the second time constant, τ_2, drops from very high values for an average Sherwood number near zero[8] to an asymtoptic value for large values. In the present case this asymtoptic value is 30.8 hours and is equal to the time constant we obtained for this case using the Equilibrium

---

[8] Recall, by equation 2.26 the second eigenvalue approaches zero for a average mass transfer coefficient, or equivalently, an average Sherwood number of zero thus the time constant becomes unbounded for a zero average Sherwood number.

Adsorption Model as predicted by Equation 3.29. ///

We may conclude, then, that, at one extreme, with a near-zero rate of diffusion mass transfer, the system will respond to changes of concentration in the zone as a simple well-mixed zone with a time constant nearly equal to (m_z/w). For nonzero rates of diffusion the system will rapidly respond to changes of concentration with a time constant somewhat less than the simple well-mixed zone time constant then, if the second mode is excited (e.g., if contaminant is generated or concentrated in the adsorbent) a very slowly changing response will be observed. Diffusion in smaller macropores and/or diffusion in micropores (e.g., having pore diameters approaching molecular sizes) may be expected to have, in essence, a similar effect to that produced by very low mass transfer rates in the BLDC Model and may be responsible for this form of observed behavior. At the other extreme, very high rates of film diffusion mass transfer lead to the simple behavior predicted by the EA Model as expected.

Surface Smoothness

The BLDC Model presumes diffusion from the zone air to a smooth surface. This begs the question: what is meant by smooth? In the present context, it would seem reasonable to define an adsorbent surface as being "smooth" (i.e., sufficiently smooth to apply the BLDC Model) if:

a) the surface roughness is small relative to the thickness of the boundary layer and

b) the structure of the surface roughness is coarser than that considered to be macroporous (i.e., the width of surface irregularities or indentations are much larger that than the mean free path of the diffusing contaminant species) so that the diffusion may be considered to be controlled by Fickian diffusion.

The thickness of the boundary layer, δ, may be estimated as [4]:

$$\delta \approx \frac{L}{Sh_L} \tag{3.32}$$

For the example considered above we obtain $\delta \approx \frac{8\ \text{m}}{27.9} = 0.29$ m which is certainly large relative to the (likely) physical roughness of the gypboard surface thus justifying the application of the BLDC Model in this case.

Adsorption Element Equations

Contaminant dispersal analysis theory may be formulated using an element assembly approach wherein equations approximating the behavior of the building airflow system or subsystem, the *system equations,* are assembled from equations that describe contaminant mass transport in discrete portions or *elements* of the system model. The details of this approach are presented elsewhere [3]. In this section we shall simply describe element equations that correspond to the adsorption models used above in the single zone case that may be used for multi-zone system models of arbitrary complexity.

In general, for the dispersal of species α, contaminant dispersal element equations have the following form:

$$[{}^{\alpha}\mathbf{w}^{e}]\{{}^{\alpha}\mathbf{C}^{e}\} + [{}^{\alpha}\mathbf{m}^{e}]\frac{d\{{}^{\alpha}\mathbf{C}^{e}\}}{dt} = \{{}^{\alpha}\mathbf{g}^{e}\} \tag{3.33}$$

where $\{{}^{\alpha}\mathbf{C}^{e}\}$ is a vector of contaminant species α discrete concentration variables associated with the element "e", a subset of *system* discrete variables $\{{}^{\alpha}\mathbf{C}\}$, and $\{{}^{\alpha}\mathbf{g}^{e}\}$ is a vector of element derived contaminant species generation rates. The element matrices $[{}^{\alpha}\mathbf{w}^{e}]$ and $[{}^{\alpha}\mathbf{m}^{e}]$ are square transformation matrices known as the element species transport matrix and species mass matrices respectively.

The element equations corresponding to the models presented above may be derived directly from Equations 3.22 by simply subtracting the single zone mass and airflow transport terms from the system equations:

Equilibrium Adsorption Element: a single node element, say element "e", with an adsorbent mass of m_S^e associated with a well mixed zone "i" with:

$$\{{}^{\alpha}\mathbf{C}^{e}\} \equiv \left\{{}^{\alpha}C_i^e\right\} \tag{3.34a}$$

$$[{}^{\alpha}\mathbf{w}^{e}] = [0] \tag{3.34b}$$

$$[{}^{\alpha}\mathbf{m}^{e}] = K_P m_S^e[1] \qquad \textit{Linear Model} \tag{3.34c}$$

or

$$[{}^{\alpha}\mathbf{m}^{e}] = \left(\frac{{}^{\alpha}C_{So}K_L}{(1 + K_L{}^{\alpha}C_i^e)^2}\right)m_S^e[1] \qquad \textit{Langmuir Model} \tag{3.34d}$$

$$\{{}^{\alpha}\mathbf{g}^{e}\} = \left\{{}^{\alpha}G_S^e\right\} \tag{3.34e}$$

Boundary Layer Diffusion Controlled Adsorption: a two node element, say element "e", associated with a well mixed zone "i" and an adsorbent "j" with an adsorbent mass of m_S^e:

$$\{{}^{\alpha}\mathbf{C}^{e}\} \equiv \left\{\begin{matrix}{}^{\alpha}C_i^e \\ {}^{\alpha}C_j^e\end{matrix}\right\} \quad ; \text{i = well-mixed zone node, j = adsorbent node} \tag{3.35a}$$

$$[^{\alpha}\mathbf{m}^e] = \begin{bmatrix} 0 & 0 \\ 0 & m_S^e \end{bmatrix} \tag{3.35b}$$

$$[^{\alpha}\mathbf{w}^e] = \left(h_m^e \, \rho \, A_S^e\right) \begin{bmatrix} 1 & \dfrac{-1}{K_P} \\ -1 & \dfrac{1}{K_P} \end{bmatrix} \qquad \textit{Linear Model} \tag{3.35c}$$

or

$$[^{\alpha}\mathbf{w}^e] = \left(h_m^e \, \rho \, A_S^e\right) \begin{bmatrix} 1 & \dfrac{-1}{K_L(^{\alpha}C_{So} - {}^{\alpha}C_j^e)} \\ -1 & \dfrac{1}{K_L(^{\alpha}C_{So} - {}^{\alpha}C_j^e)} \end{bmatrix} \qquad \textit{Langmuir Model} \tag{3.35d}$$

$$\{^{\alpha}\mathbf{g}^e\} = \begin{Bmatrix} 0 \\ ^{\alpha}G_S^e \end{Bmatrix} \tag{3.35e}$$

where all variables are defined as earlier (those variables with a following superscript "e" are specific to the adsorption element "e"). Again, note that the Langmuir Models introduce nonlinearities, now at the element level, and, for the boundary layer diffusion controlled case, are defined for adsorbent concentrations less than $^{\alpha}C_{So}$.

Implementation Using Existing Multi-Zone Programs

The Linear Models for both cases above may be implemented using existing multizone contaminant dispersal analysis programs that provide only well-mixed zones and discrete flow paths. For equilibrium adsorption modeling the analyst need only increase the associated well-mixed zone mass by $K_P m_S^e$ to account for mass transport to the adsorbent.

The boundary layer diffusion controlled case requires a slightly indirect tactic. By redefining the element concentration variables as:

$$\{^{\alpha}\mathbf{C}^e\} \equiv \begin{Bmatrix} ^{\alpha}C_i^e \\ \dfrac{^{\alpha}C_j^e}{K_P} \end{Bmatrix} \tag{3.36a}$$

the element arrays may be rewritten as:

$$[^{\alpha}\mathbf{m}^e] = \begin{bmatrix} 0 & 0 \\ 0 & K_P m_S^e \end{bmatrix} \tag{3.36b}$$

$$[{}^{\alpha}\mathbf{w}^{e}] = \left(\overline{h^{e}_{m}}\, \rho\, A^{e}_{s}\right)\begin{bmatrix} 1 & -1 \\ -1 & 1 \end{bmatrix} \qquad \textit{Linear Model} \qquad (3.36c)$$

These element equations have the form of a subassembly of a well-mixed zone linked to inflow and outflow flow elements, thus, these element equations may be added to existing multizone contaminant dispersal models by linking a pseudo-well-mixed zone to the actual well-mixed zone containing the adsorbent by two pseudo-flow paths (i.e., flow elements) having equal and opposite flows. By setting the pseudo zone mass to $K_P m^{e}_{s}$ and the pseudo-mass flows to $\left(\overline{h^{e}_{m}}\, \rho\, A^{e}_{s}\right)$ the behavior of the adsorbent will be modeled although the computed concentration response in the pseudo-well-mixed zone must be scaled by K_P to obtain the species concentration in the adsorbent, ${}^{\alpha}C^{e}_{j}$.

4
APPLICATION & VALIDATION

In this section we will consider the results of adsorption/desorption studies of formaldehyde (HCHO) on gypsum wall board reported by researchers at Oak Ridge National Labs and the National Institute of Standards and Technology. Before considering the details of these studies another study deserves mention. Cleary and Sonderagger, at Lawrence Berkeley Lab, developed a model to predict the adsorption and desorption of water in wood construction of residential attics [6, 7]. The approach taken was very similar to that developed above for the boundary layer controlled diffusion adsorption model. They combined boundary layer solutions (i.e., to model the diffusion from the bulk water concentrations to the surface of the wood construction) with an equilibrium relationship between surface and adsorbed water concentrations to form an adsorption dynamics model. The equilibrium relationship used was not one of the those presented above, instead the investigators used an empirical fit of a cubic polynomial to equilibrium data. In comparisons of modeled response to measured response of moisture levels in an attic this model proved extremely accurate.

ORNL Study

Researchers at the Oak Ridge National Labs investigated the adsorption and desorption characteristics of gypsum wall board specimens in a small test chamber and demonstrated that an empirical three-parameter exponential response model could be fitted to measured response data with reasonable accuracy. A diagram of the test set up is shown below:

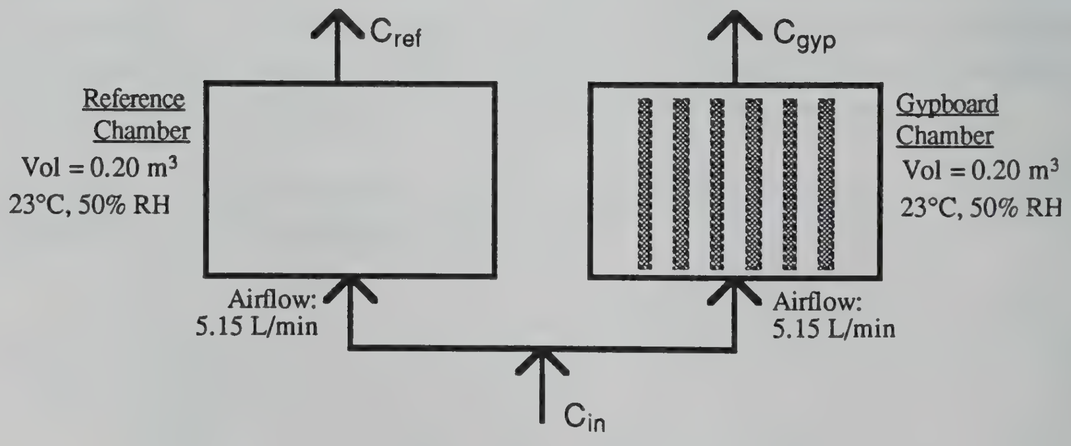

Fig. 4.1 ORNL Dual chamber test facility.

In this investigation six specimens of gypsum board (0.25m x 0.24m) were placed in one of a pair of dual test chambers (volumes of 0.20 m^3) and air, at 23° C and 50% RH, containing a controlled concentration of formaldehyde, $^{\alpha}C_{in}$, was passed through this chamber and an identical reference chamber at constant and identical rates. The exit formaldehyde concentrations from each of the chambers, ${}^{\alpha}C_{gyp}$ and ${}^{\alpha}C_{ref}$, were measured at periodical intervals and the ratio, R, of these concentrations, adjusted for initial conditions and normalized, were reported. Finally, three-parameter (i.e., A, Z, and τ) exponential relationships of the following forms:

$$R = Z + (A - Z)(1 - e^{-t/\tau}) \qquad \text{for adsorption} \qquad (4.1)$$

$$R = (A - Z)e^{-t/\tau} \qquad \text{for desorption} \qquad (4.2)$$

were fitted to measured response data. It must be emphasized, to use the words of these researchers, that "Although exponential sorption and desorption processes may represent the physical behavior of the experimental system, the precise form of the models is empirically derived."

The gypsum wall board chamber was modeled using the Linear variants of the Equilibrium Adsorption (EA) and Boundary Layer Diffusion Controlled (BLDC) models, Equations 3.9 and 3.20 proposed above, and the reference chamber was modeled as a well-mixed zone, as diagrammed below:

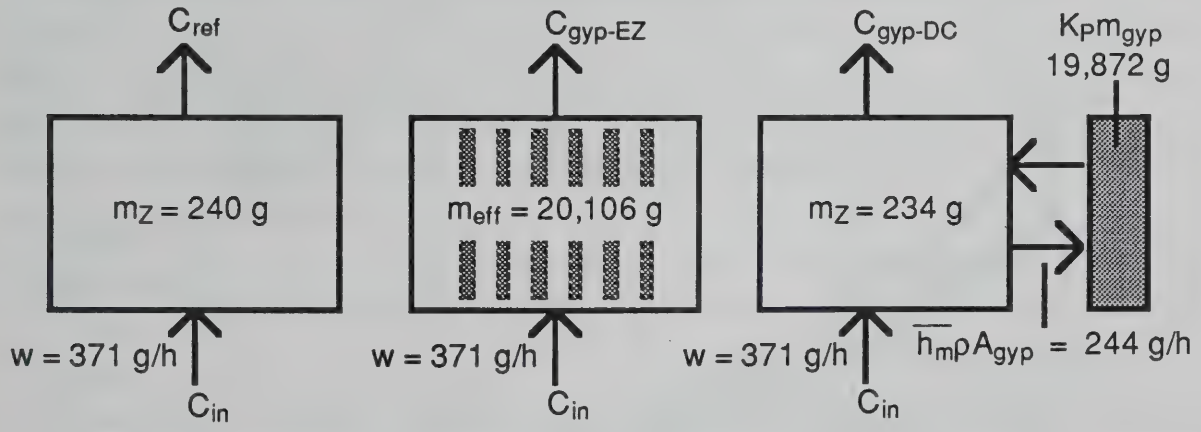

Reference Chamber Well-Mixed Model Gypboard Chamber EA Model Gypboard Chamber BLDC Model

Fig. 4.2 Idealizations of ORNL test chambers.

(For these and the following computational studies the density of the gypsum wall board was estimated to be 769,000 g/m^3, the molecular diffusivity of formaldehyde in air at 23°C was estimated to be 1.39×10^{-5} m^2/s using the Chapman-Enskog formula [5, 17], and the kinematic viscosity of air was estimated to be 1.53×10^{-5} m^2/s.)

The response of these modeled chambers was computed, using CONTAM87 [2], for a twenty eight day adsorption test followed by a four day desorption test. The results of these analyses are compared below to the ORNL empirical model along with an indication of its uncertainty (i.e., the + err and - err curves):

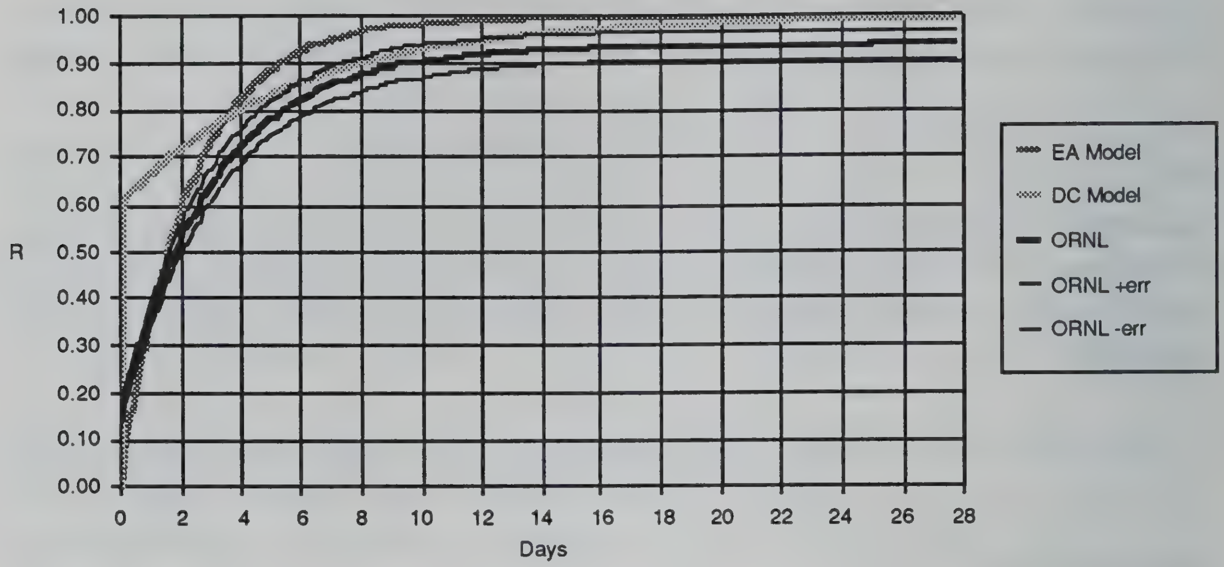

Fig. 4.3 Comparison of modeled adsorption response and ORNL empirical model.

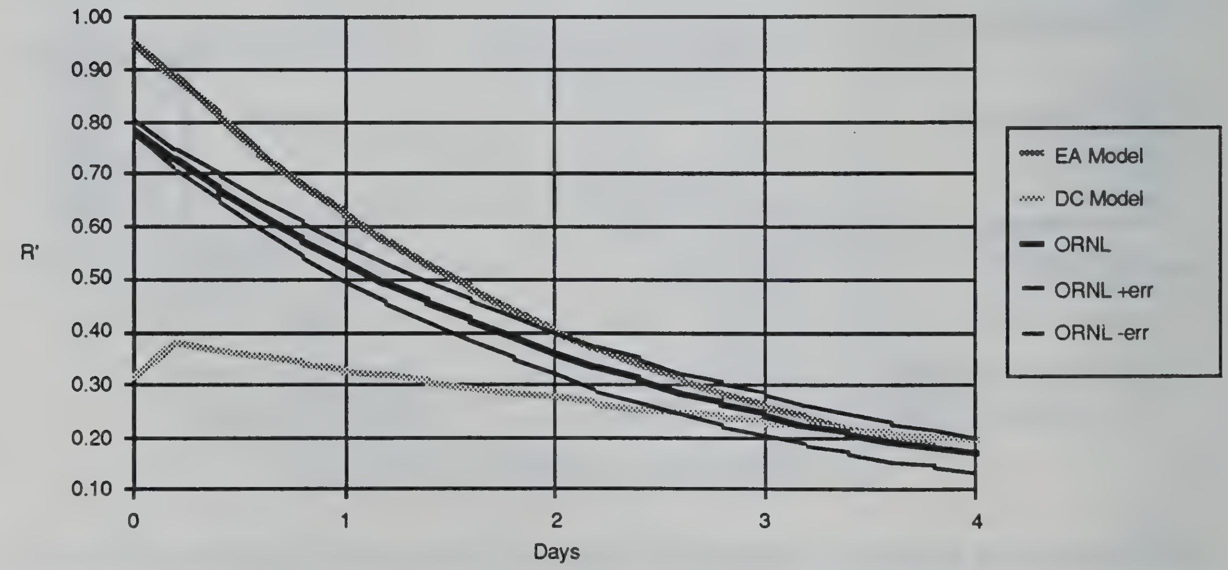

Fig. 4.4 Comparison of modeled desorption response and ORNL empirical model.

It is seen that the initial response appears to be well-captured by the EA model and the longer term response is better captured by the BLDC Model. An examination of the ORNL raw data (see Figure 3 of [12]) reveals greater scatter, especially in the bend of these curves, than the error bounds shown above indicate, thus a response falling between the EA and BLDC Models would be considered practically accurate.

The BLDC model is sensitive to the rate of diffusion mass transport that is correlated to an estimate of the flow Reynolds number. In the present case, the flow Reynolds number was based on an estimate of the mean flow velocity in the chamber equal to the volumetric flow rate divided by the square of the cube root of the chamber volume (i.e., an estimate of the chamber cross-sectional area) – more detailed information of the chamber geometry could not be obtained. This resulted in an estimate of Re = 4.25, an extremely low value; it is certain that the obstruction of the test specimens would have resulted in a larger estimate. The effect of higher Reynolds numbers (i.e., greater diffusion rates) would bring the BLDC Model curve closer to the EA Model curve in the early response and, thus improve the accuracy of the modeling.

The desorption response falls between the EA and BLDC model predictions. Again, the accuracy of the estimate of the flow Reynolds number is critical; a larger and, presumably more reasonable, Reynolds number would have improved the BLDC modeled results by "pulling" the BLDC curve closer to the EA curve.

The adsorption dynamics models presented in this report depend critically on the equilibrium adsorption isotherm model employed, in the present case, on the partition coefficient K_P. A partition coefficient of 5.5 (g-air/g-gypboard) was used for these studies and the NIST studies below. This is a value that was determined by both ORNL and NIST investigators using a rather intuitive method based on integrating the desorption response data that corresponds, in essence, to an integral form of the EA Model equations, Equations 3.9, or:

$$w\int_{t_1}^{t_2} {}^{\alpha}C_Z\,dt + (m_Z + K_P m_S)\Delta^{\alpha}C_Z = \int_{t_1}^{t_2} {}^{\alpha}E\,dt \qquad (4.3a)$$

where one integrates response and excitation values over an arbitrary time interval, $t_1 \ldots t_2$, and evaluates the change of concentration over the same interval;

$$\Delta^{\alpha}C_Z \equiv {}^{\alpha}C_Z(t_2) - {}^{\alpha}C_Z(t_1) \qquad (4.3b)$$

Solving this equation for the partition coefficient:

$$K_P = \frac{\int_{t_1}^{t_2} {}^{\alpha}E\,dt - w\int_{t_1}^{t_2} {}^{\alpha}C_Z\,dt}{m_S\,\Delta^{\alpha}C_Z} - \frac{m_Z}{m_S} \qquad (4.4)$$

defines the method used by these investigators to determine K_P (although both groups neglected to consider the second term on the right hand side, (m_Z/m_S), which was practically insignificant in both studies).

This determination of the partition coefficient implicitly assumes linear equilibrium adsorption behavior and, therefore, stacks the deck in favor of the linear equilibrium adsorption model. Silberstein, in the NIST study, also, however, used an alternate strategy to determine the partition coefficient and obtained practically identical results thereby providing some validation of the value used here. It would be best to determine this equilibrium adsorption parameter or, better, the equilibrium adsorption characteristics using one of several available independent means to do so [16].

NIST Study

In tests to study formaldehyde levels in a test house due to emissions from a variety of pressed-wood products, researchers at the National Institute of Standards and Technology found that it took days to reach equilibrium concentrations levels and suspected these long delays were due to adsorption and desorption of HCHO in gypsum wall board present in the test house [9]. To investigate this phenomena more directly these researchers conducted a separate investigation to study the adsorption and subsequent desorption of HCHO in a "medium-sized" dynamic measuring chamber, formulated a semi-empirical model of the dynamics of the sorption processes, and numerically extracted values for the model parameters from measured data [18, 19]. In distinction to the ORNL study, the environmental chamber employed was nearly room size, the gypsum board was attached to the walls of the chamber, as it would be in building construction, exposing a single side, and the proposed model was based, qualitatively, on the likely physical mechanisms responsible for adsorption. This model was not, however, directly formulated from fundamental principles of adsorption science and, therefore, must be considered a semi-empirical model.

In the NIST study a 1.2 m by 2.4 m specimen of 0.013 m thick gypsum wall board was secured to a wall of a "medium size" test chamber with inside dimensions of 1.22 m x 2.44 m x 0.61 m. This test chamber was placed in a closed environment maintained at 23° C and 50% RH, a constant fresh air flow rate through the chamber of 1.01 air changes per hour was maintained, and, for adsorption studies, formaldehyde gas was generated within the chamber at a constant rate.

The NIST chamber was modeled using the Linear variants of the Equilibrium Adsorption EA and BLDC models estimating the density of the gypsum wall board, the molecular diffusivity of the formaldehyde, and the kinematic viscosity of the air, as above, and employing the partition coefficient of 5.5 (g-air/g-gypboard). Diagrams of these models are shown below in Figure 4.5. The response of these models to an eleven day adsorption test, with formaldehyde generated within the chamber at a constant rate of 0.24 mg/h, followed by a 10 day desorption test, without the generation of formaldehyde, were computed using CONTAM87. The results of these computational analyses are compared below to the measured data, Figure 4.6.

Regrettably, there was some confusion regarding the actual formaldehyde generation rate and infiltration rate used during the test. Test data was obtained from two draft reports of the tests. In one of these reports an infiltration rate of 1.01 ACH was reported but the uncertainty associated with this value was great. The formaldehyde generation rate was reported to be 0.313 mg/hr for the adsorption tests yet hypothetical steady state concentration levels for an empty chamber were reported that indicated the actual generation rate was 0.24 mg/h; this latter value was used in the computations. Computations were based on an air exchange rate of 1.01 ACH and a generation rate of 0.24 mg/h. (Silberstein suggested, in a personal communication, that an air exchange rate closer to 1.3 ACH and the generation rate of 0.313 mg/h might be more appropriate. Since the ratios of these values are nearly identical to the values used the computed results will be very similar.)

As in the ORNL case the measured response very nearly falls between the EA Model and the BLDC Model responses. Again the BLDC response was especially sensitive to the estimation of the bulk mass transfer coefficient that was correlated with the flow Reynolds number. In this case the Reynolds number was estimated to be 110, a relatively low value. On Figure 4.6 is plotted the BLDC Model response for a ten fold increase in Reynolds number (i.e., a $\sqrt{10}$ increase in diffusion mass transfer rate) and it may be seen that the modeled response in this case more closely follows the measured response. It appears that a somewhat higher Reynolds number would have led to excellent agreement, but, at this point in time we can not provide a reliable means to estimate the flow Reynolds number accurately a priori and, therefore, the difficulty of estimating a representative Reynolds number must be considered a primary limitation of the BLDC Model approach.

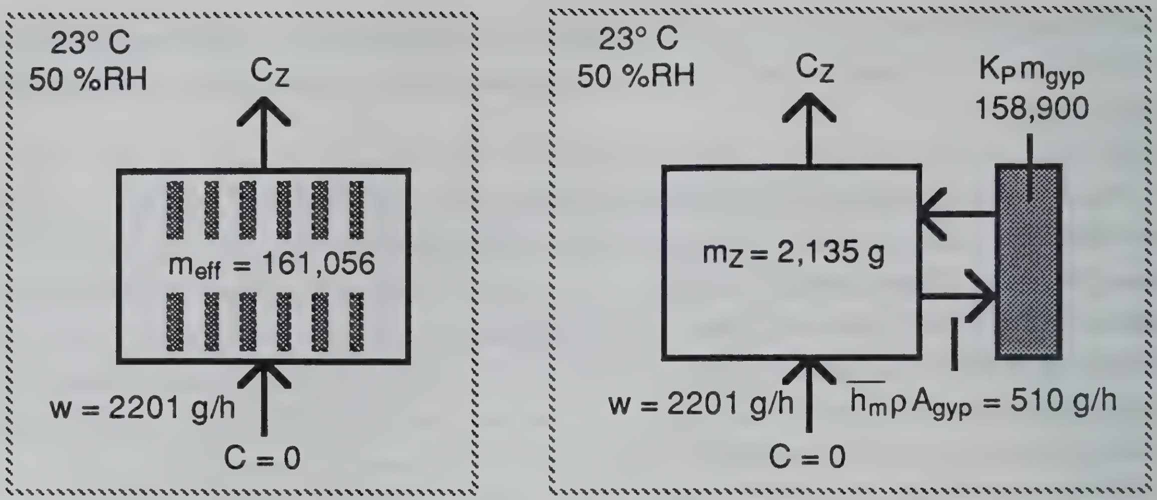

NIST Chamber
EA Model

NIST Chamber
BLDC Model

Fig. 4.5 Idealization of the NIST test chamber.

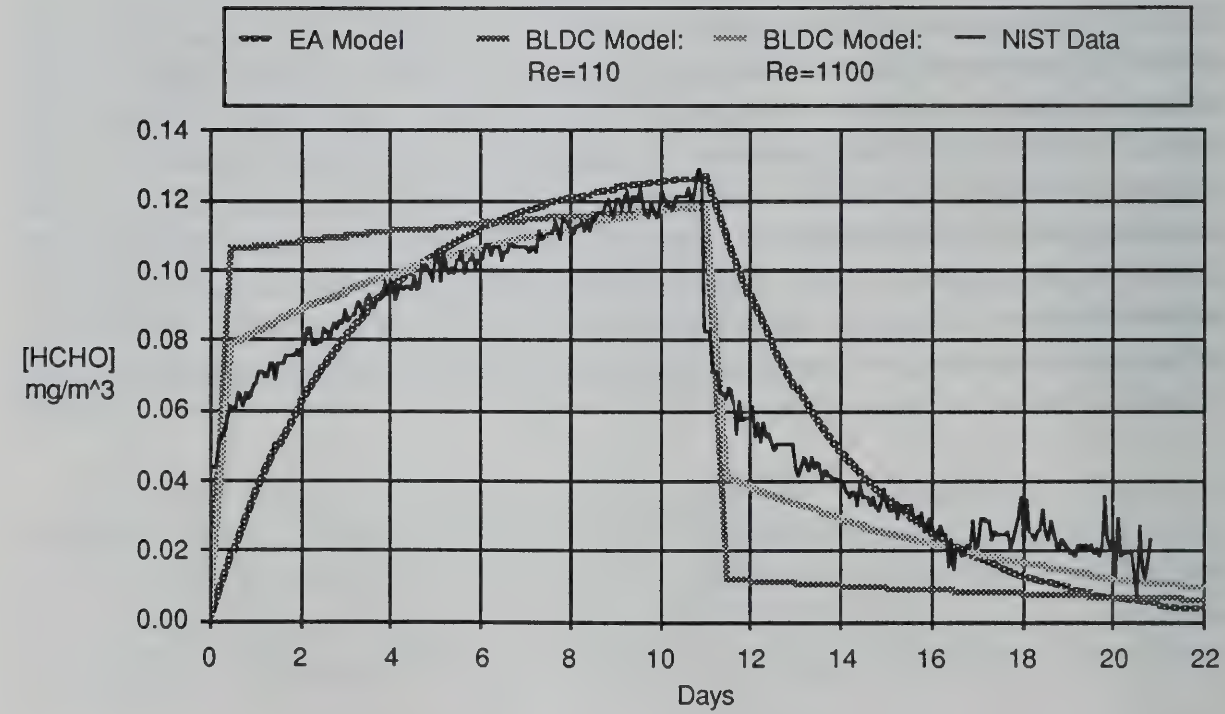

Fig. 4.6 Comparison of modeled response and NIST measured data

5

CONCLUSION

Two families of macroscopic adsorption models have been formulated, based on fundamental principles of adsorption science and technology, that may be used for the purposes of indoor air quality analysis. The first family of adsorption models – the *Equilibrium Adsorption (EA) Models* – are based upon assuming zone air concentrations and adsorbent concentrations remain in equilibrium at all times where the equilibrium condition may be defined by any number of equilibrium isotherms. Two members of this family are explicitly discussed, the first based on the linear isotherm model and the second on the Langmuir isotherm model. The second family of adsorption models – the *Boundary Layer Diffusion Controlled Adsorption (BLDC) Models* – are based on the use of boundary layer theory to model the rate of mass transfer from the bulk phase through the *boundary layer* to the solid adsorbent phase and the assumption that equilibrium exists at the solid-gas interface. Again this equilibrium may be modeled using any one of several adsorption isotherm models. Two members of this model are explicitly discussed, one based on the linear adsorption isotherm model and the other on the Langmuir model, as before.

An analysis of the linear variants of the EA and BLDC models, presented in this report, demonstrated that the EA model and the simple well-mixed zone model (i.e., without adsorbent) are simply limiting cases of the BLDC model. This analysis provides formal proof of the physical consistency of the BLDC approach.

It is shown that the linear variants of both the EA and BLDC models lead directly to contaminant dispersal *sorption elements* that may be used directly with existing contaminant dispersal analysis programs such as the CONTAM family of programs. These models have the attractive feature that they depend on a single parameter, the partition coefficient, that may be measured using one of several well-documented methods [16]. They must be expected, however, to be limited to the modeling of physical adsorption of trace contaminants because the linear adsorption isotherm upon which they are based is generally only valid for very low adsorbate concentrations. The BLDC captures the *biphasic* [18, 19] or *bimodal* nature that has been observed in adsorption and desorption tests but it relies on an estimation of the nature of airflow in the zone, as characterized by the flow Reynolds number, which, for room geometries, is a very uncertain problem. Diffusion through a boundary layer must be expected, however, to be an important step in practically all cases of adsorption and, short of complete solution of the microscopic equations governing the flow in a zone, the boundary layer solutions to this problem are the best available.

Applications of the linear variants of the EA and BLDC models to formaldehyde adsorption and desorption tests were presented to provide some first validations of these simple models. The agreement between measured and modeled response was excellent. These practical applications and the example applications considered to clarify the development of the models clearly indicate the significant, in fact, overwhelming affect that simple physical adsorption and desorption transport processes may have on the dispersal of contaminants in buildings. Furthermore, physical adsorption must be expected to be pervasive depending not so much on special characteristics of adsorbate-adsorbent systems but simply on the availability of sufficient adsorbent surface. To date, sorption processes have been largely ignored in indoor air quality analysis and, importantly, in the closely related field of tracer gas analysis of building airflows. Both areas of analysis should be reevaluated in light of the implications of the results reported here.

The success of the work reported by Cleary and his colleagues [6, 7] in modeling moisture variation in wood construction supports the hope that the nonlinear variants (e.g., Langmuir and BET adsorption isotherms) of the EA and BLDC models will prove effective in modeling physical sorption mass transport when adsorbate concentrations vary over wide ranges and may not be at trace levels (e.g., moisture variations in buildings in general), but this will have to be investigated.

Not presented in this report are physical adsorption and desorption models based on existing knowledge of macro and microporous diffusion processes. It is clear, however, that macroscopic models could be readily developed based on finite element approximations to available governing differential equations for these classes of diffusion (e.g., the so-called Glueckauf Model for the diffusive transport of an adsorbate down a cylindrical pore in a macroporous adsorbent [10]). The numerical studies reported clearly indicate the potential importance of diffusion rate limitations – diffusion resistance can lead to extremely long time constants in adsorption dynamics. It is entirely possible that the exponentially-diminishing "source" models reported by some investigators and the apparent irreversible, but small, conversion of formaldehyde in gypsum wall board are both due to more deeply adsorbed (e.g., within macro or microporous structures) constituents. It seems likely that a consideration of these more rate limiting diffusion steps in the adsorption process may lead to some rationally based physical "source" models.

6
REFERENCES

1. Andelman, J. B., N. J. Giardino, J. Marshall, N. A. Esmen, J. E. Borrazzo, C. I. Davidson, M. Small and C. Wilkes. Exposure to Volatile Chemicals from Indoor Uses of Water. Symposium: Total Exposure Methodology: A New Horizon. 1989.

2. Axley, J. W. Progress Toward a General Analytical Method for Predicting Indoor Air Pollution in Buildings: Indoor Air Quality Modeling Phase III Report. NBSIR 88-3814. U.S. DOC, NBS, Gaithersburg, MD. 1988.

3. Axley, J. W. Multi-Zone Dispersal Analysis by Element Assembly. Building and Environment. Vol. 24, No. 2: pp. 113-130, 1989.

4. Beek, W. J. and K. M. K. Muttzall. "Transport Phenomena." 1975 John Wiley & Sons, Ltd. London.

5. Bird, R. B., W. E. Stewart and E. N. Lightfoot. "Transport Phenomena." 1960 John Wiley & Sons, Inc. New York.

6. Cleary, P. and M. Sherman. Seasonal Storage of Moisture in Roof Sheathing. LBL-17774. Lawrence Berkeley Laboratory, Applied Science Division. 1984.

7. Cleary, P. and R. Sonderegger. A Method to Predict the Hour by Hour Humidity Ratio of Attic Air. LBL-17591. Lawrence Berkeley Laboratory, Applied Science Division. 1984.

8. Ethier, C. R. and R. D. Kamm. Mass Transfer During Rate-Limited Langmuir Adsorption in a Pore. Physiochemical Hydrodynamics. Vol. 11(No. 2): pp. 205-217, 1989.

9. Grot, R. A., S. Silberstein and K. Ishiguro. "Validation of Models for Predicting Formaldehyde Concentrations in Residences Due to Pressed Wood Products: Phase I." 1985 U.S. D.O.C., NBS, NEL, CBT. Gaithersburg, Md.

10. Holland, C. D. and A. I. Liapis. "Computer Methods for Solving Dynamic Separation Problems." 1983 McGraw-Hill Book Co. New York.

11. Jaroniec, M. and R. Madey. "Physical Adsorption on Heterogeneous Solids." 1988 Elsevier. Amsterdam.

12. Matthews, T. G., A. R. Hawthorne and C. V. Thompson. Formaldehyde Sorption and Desorption Characteristics of Gypsum Wallboard. Environmental Science and Technology. Vol. 21(No. 7): pp. 629-634, 1987.

13. Oscik, J. and I. L. Cooper. "Adsorption." 1982 Halsted Press. New York.

14. Ponec, V., Z. Knor and S. Cerny. "Adsorption on Solids." 1974 CRC Press. Cleveland.

15. Rodrigues, A. E., M. D. LeVan and D. Tondeur. Adsorption: Science and Technology. 591 pages, 1988.

16. Ruthven, D. M. "Principles of Adsorption and Adsorption Processes." 1984 John Wiley & Sons. New York.

17. Satterfield, C. N. "Mass Transfer in Heterogeneous Catalysis." 1970 MIT Press. Cambridge, MA.

18. Silberstein, S. A Gypsum Wallboard Formaldehyde Sorption Model. DRAFT: NISTIR. NIST. 1988.

19. Silberstein, S. A Gypsum Wallboard Formaldehyde Sorption Model. DRAFT: NISTIR. NIST. 1989.

20. Slejko, F. L. Adsoprtion Technology: A Step-by-Step Approach to Process Evaluation and Application. 1985.

21. White, F. M. "Heat and Mass Transfer." 1988 Addison-Wesley Pub. Co. New York.

NIST-114A
(REV. 3-89)

U.S. DEPARTMENT OF COMMERCE
NATIONAL INSTITUTE OF STANDARDS AND TECHNOLOGY

BIBLIOGRAPHIC DATA SHEET

1. PUBLICATION OR REPORT NUMBER
NIST-GCR-90-573

2. PERFORMING ORGANIZATION REPORT NUMBER

3. PUBLICATION DATE
MAY 1990

4. TITLE AND SUBTITLE

Adsorption Modeling for Macroscopic Contaminant Dispersal Analysis

5. AUTHOR(S)

James W. Axley

6. PERFORMING ORGANIZATION (IF JOINT OR OTHER THAN NIST, SEE INSTRUCTIONS)

Building Technology Program
Massachusetts Institute of Technology
Cambridge, Massachusetts

7. CONTRACT/GRANT NUMBER
43NANB919513

8. TYPE OF REPORT AND PERIOD COVERED

9. SPONSORING ORGANIZATION NAME AND COMPLETE ADDRESS (STREET, CITY, STATE, ZIP)

National Institute of Standards and Technology
Gaithersburg, MD 20899

10. SUPPLEMENTARY NOTES

☐ **DOCUMENT DESCRIBES A COMPUTER PROGRAM; SF-185, FIPS SOFTWARE SUMMARY, IS ATTACHED.**

11. ABSTRACT (A 200-WORD OR LESS FACTUAL SUMMARY OF MOST SIGNIFICANT INFORMATION. IF DOCUMENT INCLUDES A SIGNIFICANT BIBLIOGRAPHY OR LITERATURE SURVEY, MENTION IT HERE.)

Two families of macroscopic adsorption models are formulated, based on fundamental principles of adsorption science and technology, that may be used for macroscopic (e.g., whole-building) contaminant dispersal analysis. The first family of adsorption models - the Equilibrium Adsorption (EA) Models - are based upon the simple requirement of equilibrium between adsorbent and room air. The second family - the Boundary Layer Diffusion Controlled Adsorption (BLDC) Models - add to the equilibrium requirement a boundary layer model for diffusion of the adsorbate from the room air to the adsorbent surface. Two members of each of these families are explicitly discussed, one based on the linear adsorption isotherm model and the other on the Langmuir model. The linear variants of each family are applied to model the adsorption dynamics of formaldehyde in gypsum wall board and compared to measured data.

12. KEY WORDS (6 TO 12 ENTRIES; ALPHABETICAL ORDER; CAPITALIZE ONLY PROPER NAMES; AND SEPARATE KEY WORDS BY SEMICOLONS)

adsorption; contaminant dispersal; indoor air quality; modelling

13. AVAILABILITY

☒ **UNLIMITED**
☐ **FOR OFFICIAL DISTRIBUTION. DO NOT RELEASE TO NATIONAL TECHNICAL INFORMATION SERVICE (NTIS).**
☐ **ORDER FROM SUPERINTENDENT OF DOCUMENTS, U.S. GOVERNMENT PRINTING OFFICE, WASHINGTON, DC 20402.**
☒ **ORDER FROM NATIONAL TECHNICAL INFORMATION SERVICE (NTIS), SPRINGFIELD, VA 22161.**

14. NUMBER OF PRINTED PAGES
42

15. PRICE
A03

ELECTRONIC FORM